NUREG/CR-2189, Vol. 3
UCID-18967, Vol. 3
RM

NUREG/CR--2189-Vol.3

TI85 016044

Probability of Pipe Fracture in the Primary Coolant Loop of a PWR Plant

Volume 3: Nonseismic Stress Analysis Load Combination Program Project I Final Report

Manuscript Completed: June 1981
Date Published:

Prepared by
A. L. Chan, S. C. Lu, E. F. Rybicki, D. J. Curtis

Lawrence Livermore Laboratory
7000 East Avenue
Livermore, CA 94550

Prepared for
Division of Engineering Technology
Office of Nuclear Regulatory Research
U.S. Nuclear Regulatory Commission
Washington, D.C. 20555
NRC FIN No. A-0133

Blank Page

ABSTRACT

This volume describes the analyses used to evaluate stresses due to loads other than seismic excitations in the primary coolant loop piping of a selected four-loop pressurized water reactor nuclear power station. The results of the analyses are used as input to a simulation procedure for predicting the probability of pipe fracture in the primary coolant system.

Sources of stresses considered in the analyses are pressure, dead weight, thermal expansion, thermal gradients through the pipe wall, residual welding, and mechanical vibrations. Pressure and thermal transients arising from plant operations are best estimates and are based on actual plant operation records supplemented by specified plant design conditions.

Stresses due to dead weight and thermal expansion are computed from a three-dimensional finite element model that uses a combination of pipe, truss, and beam elements to represent the reactor coolant loop piping, reactor pressure vessel, reactor coolant pumps, steam generators, and the pressurizer. Stresses due to pressure and thermal gradients are obtained by closed-form solutions. Calculations of residual stresses account for the actual heat impact, welding speed, weld preparation geometry, and pre- and post-heat treatments. Vibrational stresses due to pump operation are estimated by a dynamic analysis using existing measurements of pump vibrations.

Blank Page

CONTENTS

Blank Page

LIST OF FIGURES

LIST OF TABLES

EXECUTIVE SUMMARY

The Code of Federal Regulations requires that structures, systems, and components that affect the safe operation of nuclear power plants be designed to withstand combinations of loads that can be expected to result from natural phenomena, normal operating conditions, and postulated accidents. One load combinations requirement--the combination of the most severe LOCA (loss-of-coolant accident) load and SSE (safe shutdown earthquake) loads--has been controversial because both events occur with very low probabilities. This issue became more controversial in recent years because postulated large LOCA and SSE loads were each increased by a factor of 2 or more to account for such phenomena as asymmetric blowdown and because better techniques for defining loading have been developed.

The original objective of Load Combinations Project I was to estimate the joint probability of simultaneous occurrence of both events and to develop a technical basis for the NRC (Nuclear Regulatory Commission) to use in determining whether it could relax its requirement on the combination of SSE and large LOCA for nuclear power plants. However, in the process of probability estimation we have not only estimated the probability of simultaneous occurrence of a large LOCA and an earthquake, but also estimated the probability of a large LOCA caused by normal and abnormal loading conditions without an earthquake. The estimates provide very useful information on the likelihood of asymmetric blowdown, which is a subset of large LOCA. Also, the probabilistic fracture mechanics model that we developed can be used to estimate the probability of pipe rupture with or without prior leak. That is, we can estimate the proportion of pipes that will leak detectably before rupture under normal operation, accident, or upset conditions. We can also evaluate the piping reliability in general. After a sufficient parametric study is done, we will be able to recommend a more rational basis for postulating pipe rupture locations.

If earthquakes and large LOCAs are independent events, the probability of their simultaneous occurrence is small. However, this probability is expected to be greater if an earthquake can induce pipe failure that leads to a LOCA. This LOCA could result directly (i.e., ground motion causes a pipe break in the primary cooling system) or indirectly (e.g., an earthquake causes a structural, mechanical, or electrical failure that in turn causes a pipe break in the primary cooling system).

In the first-phase study reported in these nine volumes, we concentrated on determining the probability of a large LOCA in a PWR plant directly induced by an earthquake. The expert consensus is that such a directly induced LOCA is most likely to result from the growth of cracks formed in the pipes during fabrication. We selected a demonstration plant for study (Unit 1 of the Zion Nuclear Power Plant), modeled its primary cooling loop (Vol. 2), analyzed the best estimated responses of that piping system to nonseismic and seismic stresses (Vols. 3 and 4), developed a probabilistic fracture mechanics model of that piping system (Vols. 5, 6, and 7), analyzed failure mode (Vol. 6) and developed a computer code, PRAISE, to simulate the life history of a primary coolant system (Vol. 9). Finally, we examined the probability with which an earthquake can indirectly induce a LOCA (Vol. 8).

In Volume 3, we present our analysis of the best estimated responses of the piping system to nonseismic stresses. The relation between this volume and the rest of the report is shown in the following drawing:

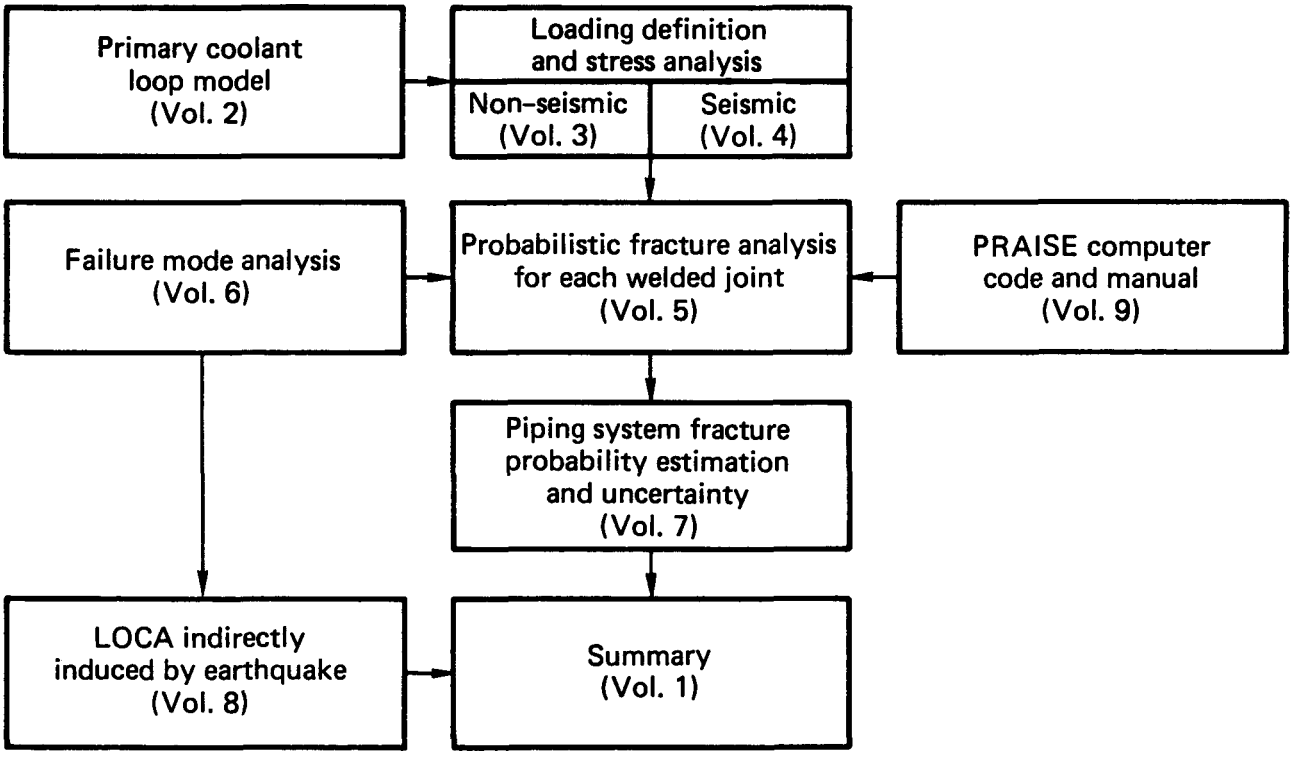

1.0 INTRODUCTION

This volume describes the nonseismic stress calculation methods and results for the primary coolant loop piping system for the Zion Unit 1 nuclear plant. The resulting streses are used to predict the probability of stress-induced pipe fracture at the circumferential welded joints. The following types of stresses are treated in this study:

- Thermal-expansion and dead-weight stresses
- Pressure stresses
- Thermal gradient stresses
- Residual stresses due to welding
- Mechanical vibration stresses.

Seismic stresses are not included in this volume because they are covered in Volume 4.

In a normal piping design procedure, the usually conservative design conditions are used for the pipe stress analyses. In this study, the objective is to use data that will best reflect the actual plant operating conditions. For the Zion nuclear plant, temperatures and pressures for various thermal and pressure transients are recorded in the form of strip charts and computer printouts during plant operation. Data are available for the following transients:

1. Heat up
2. Cool down
3. Unit loading at 5% per minute
4. Unit unloading at 5% per minute
5. 10% load increase
6. 10% load decrease (with steam dump)
7. 10% load decrease (without reactor trip).

8. Reactor trip from full power
9. Large load decrease (with steam dump)
10. Loss of flow
11. Loss of power.

After careful evaluation of the recorded data, we found that the recording time steps of the majority of the strip charts from the computer printouts are too far apart to fully describe the thermal transients except for the first four transients listed above. For example, the recording time step is 5 minutes for the reactor-trip transient, where the most severe temperature change occured within the first 100 seconds of the transient. However, useful information can be obtained from the transient data for unit loading and unloading at 5% per minute. Figure 1-1 plots temperature vs percentage reactor power for these two transients. A straight line is drawn through the data points by the least square fitting method to determine the operating temperatures for the hot and cold legs. The * designates the data obtained from strip charts and O designates data obtained from the computer printout. We may note that the data from the strip chart is highly irregular. Therefore, only data from the computer printout are used for the least square fitting. The temperatures for the full power and hot standby conditions are:

Hot standby:	Cold leg	=	548.5 ^{o}F
	Hot leg	=	548.5 ^{o}F
Full power:	Cold leg	=	588 ^{o}F
	Hot leg	=	540 ^{o}F.

These temperatures are used for the analyses of thermal expansion and thermal radial gradient stress. For a comparison, the design temperature for the hot standby condition is 547 ^{o}F, and the design temperatures for the full power condition are 592 ^{o}F and 530 ^{o}F for the hot and cold legs, respectively.

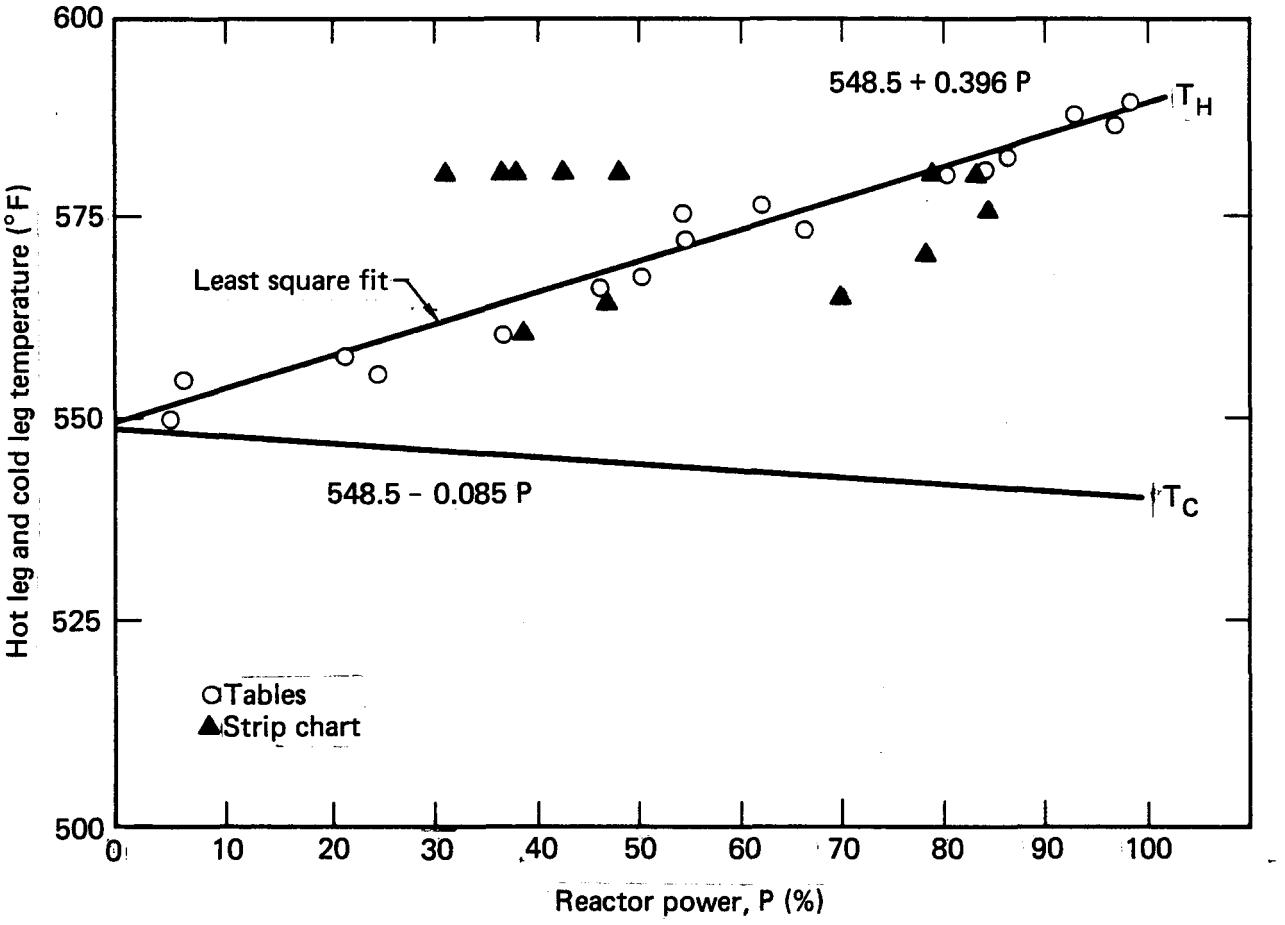

FIG. 1-1. Unit loading and unloading at 5% per minute transient data (from Zion Unit 1 operating record).

2.0 THERMAL-EXPANSION, DEAD-WEIGHT, AND PRESSURE STRESS ANALYSES

This section describes the methods and results of the thermal-expansion, dead-weight, and pressure stress calculations of the primary coolant piping system. Thermal expansion stress is defined as the stress induced by limiting the thermal expansion and contraction of the piping system. Dead-weight stress is caused by the piping system's own weight, and pressure stress is produced by internal pressure loading of the piping system.

The thermal-expansion and dead-weight stresses are computed using the SAP4 finite element computer program.[1] The pipes, reactor pressure vessel, steam generators, reactor coolant pumps, pressurizer, valves, and component supports are represented in the SAP4 finite element model by the combination of pipe, beam, and truss elements. All four loops are modeled in the analysis. The finite element model is a modified version of a model developed by Sargent & Lundy Engineers for seismic analyses. Both the seismic and the nonseismic finite element models are described in detail in Volume 2 of this report. Only the major modifications will be discussed.

Truss Elements

Modulus of elasticity of four member properties was taken out. This has the effect of making the corresponding supports inactive (zero stiffness). These changes make all snubber supports inactive for all static loads. Member property 1 represents the snubbers acting in the radial direction of the steam generator upper lateral support. Member properties 5, 6, and 7 represent surge line seismic supports RCRS-1007, RCRS-1008, and RCRS-1009, respectively. RCRS-1008 is a seismic sway strut. A slotted hole connection is provided at one end of the strut to ensure that the support does not carry static loads.

Beam Elements

a. Material Property

A second material property has been added so that supports may be separated into two categories. Material property 1 is for weightless supports, and material property 2 is for supports with effective weight. In many cases, lateral supports are cantilevered off a wall and do not cause static loads to act on the reactor coolant system. The weight of vertical supports is included for completeness but may be excluded as described below.

b. Element Load Factors

A factor of -1.0 is used for gravity load in the +Z direction. The weight of vertical supports may be taken out of the analysis simply by setting this factor equal to zero.

c. Beam Element Data

The material property number was changed to 2 for steam generator columns (beam Nos. 1, 2, 3, and 4), reactor coolant pump columns (Nos. 13, 14, 15, and 16), pressurizer columns (No. 25), and pipe clamps on the surge line (Nos. 32 and 33).

Axial stiffness of several beam elements is made inactive by adding member releases. The steam generator lower lateral support is inactive in the radial direction (beam Nos. 9, 10, 11, and 12). Both the tangential and the radial reactor coolant pump supports (Nos. 17 through 24) are provided with slotted end connections to make them inactive for static loads.

The torsional stiffness in the reactor coolant pump columns (Nos. 13 through 16) becomes zero because this stiffness is actually provided by the lateral supports, which are inactive for static loads.

Finally, the surge line flailing restraints are completely isolated by large gaps, and thus are totally released at the pipe and fixed at the wall.

Pipe Elements

a. Material Property

Material properties are reorganized into eight groups for static analysis, as shown in Table 2-1.

b. Section Property

The weight per unit length in pounds per lineal foot was added for all straight pipes, elbows, and horizontal valve sections. All remaining weights are input as concentrated nodal loads.

c. Pipe Element Data

The average internal operating pressure of 321,800 psf (2235 psi) has been applied to all straight pipe and elbows. Also, the section property identification number for elements representing the pipe and the valve in the cold leg has been changed to 8. These elements are numbered 39-50, 89-100, 139-150, and 189-200.

d. Concentrated Nodal Load Data

Equipment weights and preset hanger loads are input to the model as concentrated loads. These loads are itemized in Table 2-1. All loads are entered twice so that they are considered in both load combination 1 (weight) and combination 3 (weight plus thermal).

The input temperatures for the thermal expansion analysis are 588 ^{o}F for the hot leg and 540 ^{o}F for the cold leg and the cross-over. For the surge line, the average temperature between the hot leg and the pressurizer (653 ^{o}F) is used. The stress results are plotted in Figs. 2-1 and 2-2, for the loop 1 thermal-expansion and dead-weight stresses respectively. Figure 2-3 shows the Zion nuclear steam supply system, including the joint numbers. The stresses shown in this volume are the maximum principal stresses. They are calculated with the following equation:

$$\sigma_{1,\,2} = \text{principal stresses} = \frac{\sigma_B+\sigma_T}{2} \pm \sqrt{\left[\frac{\sigma_B+\sigma_T}{2}\right]^2 + \tau^2}$$

$$\text{where } \sigma_B = \text{bending stress} = \sqrt{\frac{M_z^2+M_y^2}{Z}}$$

τ = torsional shear stress

σ_T = axial stress = F/A

M_y = bending moment in the Y axis

M_z = bending moment in the Z axis

F = axial force

A = cross sectional areas of pipe

Z = section modulus.

The longitudinal and hoop stresses due to internal pressure are obtained from the following formulas:

$$\sigma_L = \frac{PD}{4H}$$

$$\sigma_H = \frac{PD}{2H}$$

where

σ_L = longitudinal stress

σ_H = hoop stress

P = internal pressure

D = pipe outside diameter

H = pipe thickness.

A summary of stresses due to internal pressure is given in Table 2-2.

Table 2-1. Material properties

Property No.	Component	Modulus of elasticity ($X10^9$ psf)	Coefficient of thermal expansion ($X\ 10^{-6}$ in./in.^oF)
1	Steam generator and pressurizer	3.800	7.18
2	Reactor pressure vessel	3.715	9.74
3	Hot leg and surge line	3.730	9.82
4	Hot leg valve	3.860	9.47
5	Steam generator inlet nozzle	3.790	7.18
6	Crossover leg and reactor coolant pump casing	3.770	9.74
7	Reactor coolant pump motor	4.020	6.19
8	Cold leg and cold leg valve	3.800	9.74

Table 2-2. Stresses due to internal pressure

Pipe segment	Pressure (psi)	O.D. (in.)	Thickness (in.)	Long. stress (psi)	Hoop stress (psi)
Hot leg	2235	34.0	2.50	7600	15200
Crossover	2235	36.3	2.66	7630	15250
Cold leg	2235	32.3	2.38	7580	15170

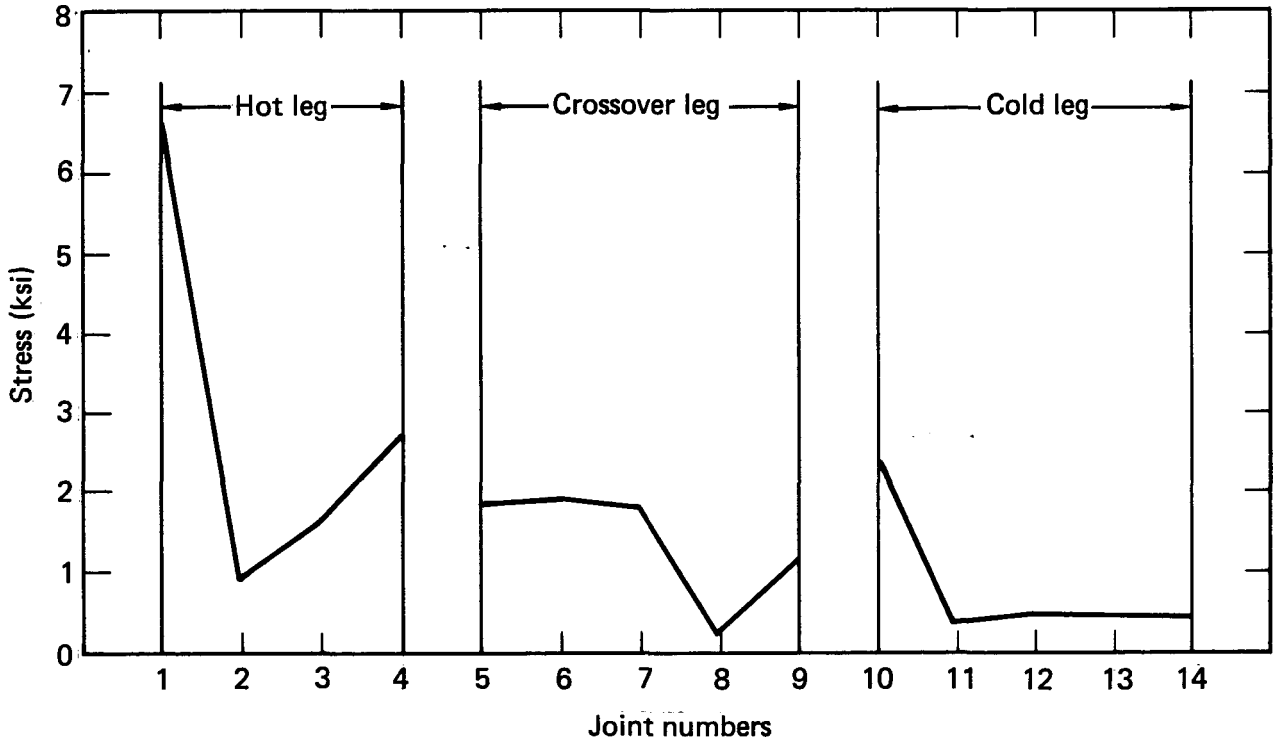

FIG. 2-1. Thermal expansion stresses at primary coolant loop welded joints. (For locations of joint numbers, see Fig. 2-3.)

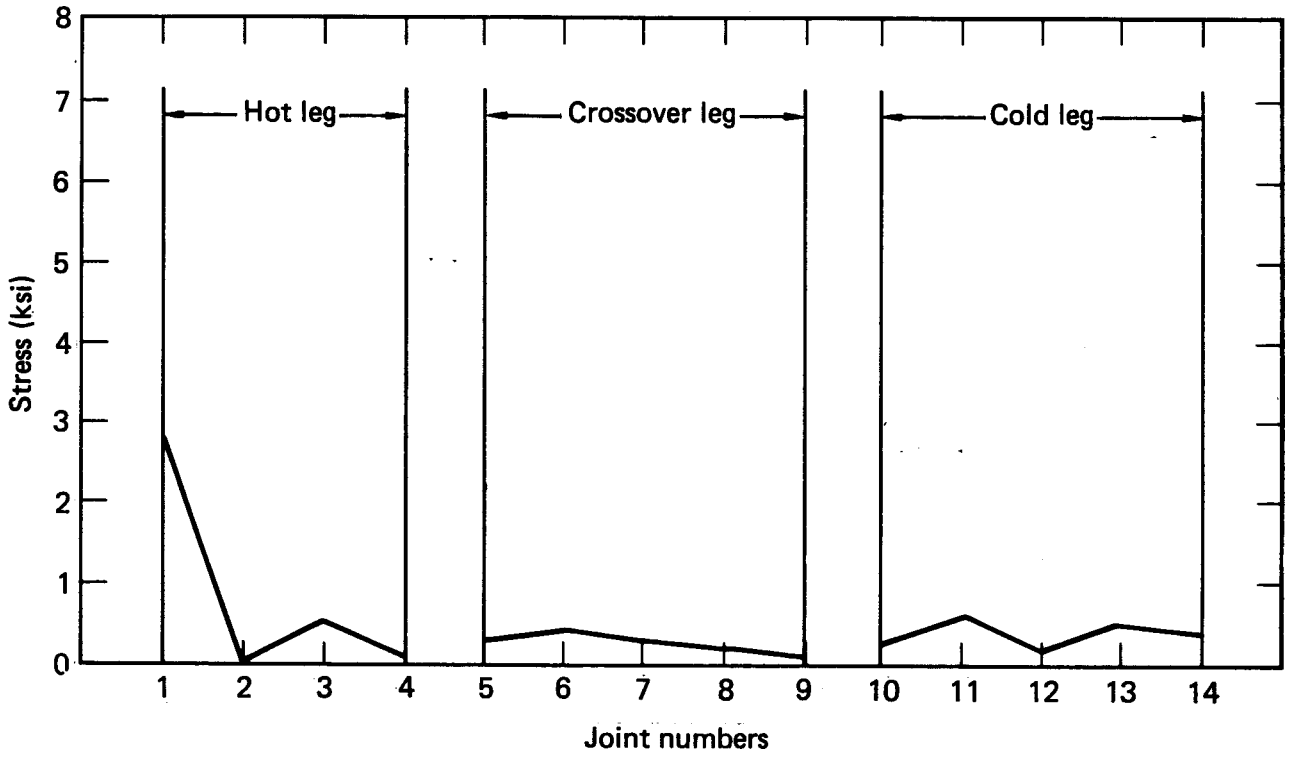

FIG. 2-2. Dead-weight stresses at primary coolant loop welded joints. (For locations of joint numbers, see Fig. 2-3.)

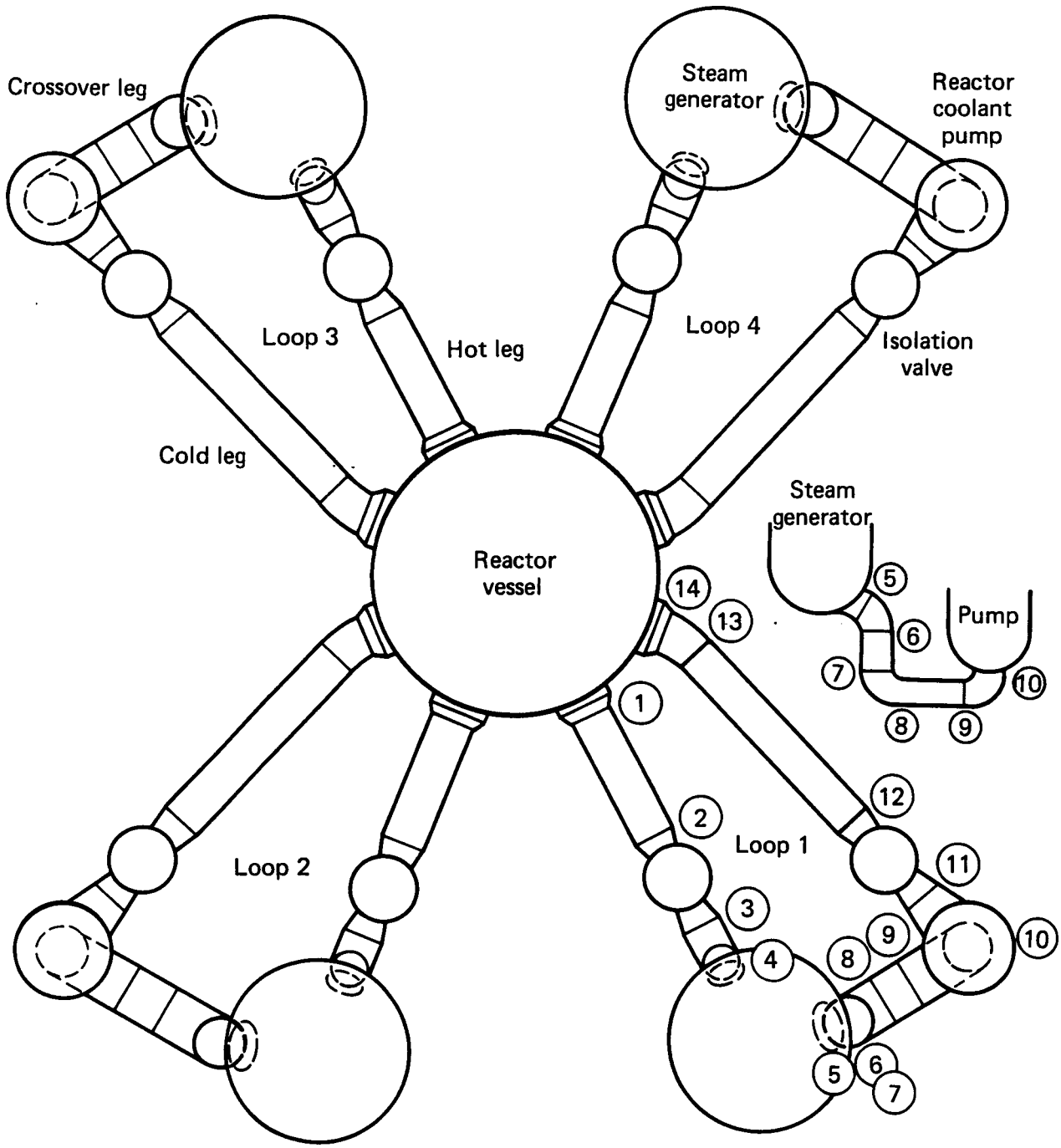

FIG. 2-3. Zion-1 nuclear steam supply; circled numbers indicate joint numbers.

3.0 THERMAL GRADIENT STRESSES

During a thermal transient condition, the change in fluid temperature creates a non-uniform temperature distribution across the pipe wall. This temperature distribution induces non-uniform across-the-pipe-wall stresses that are referred to as thermal gradient stresses. The thermal gradient stresses have been calculated for the hot leg, cold leg, and surge line. The cross-over is not evaluated because its wall thickness is similar to that of the cold leg and also because it will experience the same thermal transient as the cold leg. Therefore, the resulting thermal gradient stresses for the cold leg will also be used to evaluate the cross-over. The pipe dimensions analyzed are shown in Table 3-1. The 4-in.-thick portion represents the thickness of the isolation valves in the hot and cold legs.

3.1 TRANSIENT DATA

The original intention of this study was to use Zion-recorded fluid temperature data to analyze the thermal transient stresses. However, the large time step of the recorded computer printout made it difficult to determine the temperature histories accurately during a particular transient. Therefore, the Westinghouse design transient curves[2] are used for the thermal gradient stress analyses. During the evaluation of the thermal gradient stresses it was noticed that for some transients, minimum and maximum values at the pipe surface tended to occur after or at the time limit shown by the Westinghouse curve. Since the termperature changes across the pipe thickness had not actually terminated by this time limit, the given curves were extrapolated. In most cases, the final coolant temperature given in the Westinghouse curves was extrapolated out to a sufficient time to see 5% change in the inside-surface thermal stress. The only exception to this procedure is the steam line break transient, where the eventual temperature is 212 ^{o}F for both hot leg and cold legs. The extrapolation for this case is made linearly to 212 ^{o}F.

Thirteen thermal transients are evaluated for this study. They are listed in Table 3-2. The temperature input for each type of transient is given in Appendix A of this volume.

Table 3-1. Pipe dimensions.

Leg	Pipe i.d. (in.)	Pipe thickness (in.)
Hot	29	2.5
	29	4
Cold	27.5	2.38
	27.5	4
Surge line	11.19	1.406

Table 3-2. Description of transients analyzed for the cold and hot legs.

Transient No.	Description
1	Reactor heatup
2	Reactor cool down
3	Plant loading, 5% per minute
4	Plant unloading, 5% per minute
5	10% step load decrease
6	10% step load increase
7	Large step decrease in load
8	Loss of load from full power
9	Loss of offsite power
10	Loss of flow in one loop, the last loop
11	Loss of flow in one loop, the other loops
12	Reactor trip from full power
13	Steam line break from zero power

3.2 PIPE PROPERTIES

The following properties were used in the analysis:

E = (Young's modulus) = 2.83×10^7 psi

α = (thermal expansion coefficient) = 9.1×10^{-6}

D = (thermal diffusibility in ft^2/hr) = $0.1468 + 0.00000387\ T$

k = (thermal conductivity in Btu/ft-hr-^oF) = $8.0 + 0.004381\ T$

where T is the time-averaged coolant temperature in ^oF.

3.3 MATHEMATICAL METHOD

Thermal gradient stresses existing in the pipe wall can be resolved into axial, hoop, and radial components. For the purpose of investigating pipe fracture at a circumferentially welded joint, only the axial component of the thermal gradient stress needs to be computed.

The axial stress $\sigma_Z(r,t)$ induced by the thermal gradient at any time t in a circular pipe having an inner radius a and an outer radius b can be determined by the following equation[3]:

$$\sigma_Z = \frac{E\alpha}{1-\nu}\left[\frac{2\nu}{b^2-a^2}\int_a^b Trdr - T\right] + \frac{2E\alpha}{b^2-a^2}\int_a^r Trdr, \qquad (3\text{-}1)$$

where r is a spatial variable defining the position (radius) of the point of interest in the pipe wall, ν is the Poisson's ratio of the pipe material, and $T(r,t)$ is the local pipe temperature at the instance of interest. $T(r,t)$, in turn, can be determined by solving the classical initial-boundary value problem that is governed by the heat conduction equation[4]

$$\frac{\partial^2 T}{\partial r^2} + \frac{1}{r}\frac{\partial T}{\partial r} = \frac{1}{D}\frac{\partial T}{\partial \tau} \qquad (3\text{-}2)$$

Equation (3-2) is subject to the prescribed initial condition at the beginning

of the problem as well as boundary conditions at the inner and outer pipe wall, i.e., r = a and r = b, respectively. These boundary conditions are

$$\frac{\partial T}{\partial r} = \frac{h}{k} (T_c - T) \text{ at } r = a ,$$

$$\frac{\partial T}{\partial r} = 0 \qquad \text{at } r = b , \tag{3-3}$$

where h is the heat transfer coefficient between the coolant and the pipe wall and T_c, a function of time t, is the instantaneous coolant temperature. The initial condition is such that the temperature in the pipe wall at t = 0 equals the initial coolant temperature, i.e.,

$$T(r,0) = T_c(0), \text{ for } a \leq r \leq b . \tag{3-4}$$

A closed-form solution of the above initial-boundary value problem exists if k, D, and h are constant, i.e., independent of the temperature. However, the closed-form solution cannot be applied here because the heat transfer coefficient h can vary between 6000 and 1.0 Btu/ft-hr-^{o}F for the surge line in a very short period of time. Thus, a numerical approach has to be employed. In this study, a finite difference method has been adopted in order to obtain the transient temperature distribution in the pipe wall.

3.4 RESULTS AND DISCUSSION

The time-variant stress distributions for each transient are calculated by the method described in Section 3.3. The results are stored on tape for retrieval later for stress-intensification-factor calculations. A typical stress distribution for the hot leg is shown in Fig. 3-1. The temperature transient is described in Fig. 3-2. The stress results are summarized in Tables 3-3 and 3-4. These tables indicate the maximum and minimum stresses at the inside surface of the pipe and the time they occur. It must be pointed out that the maximum stress intensity does not necessarily appear at the same time as the maximum stress.

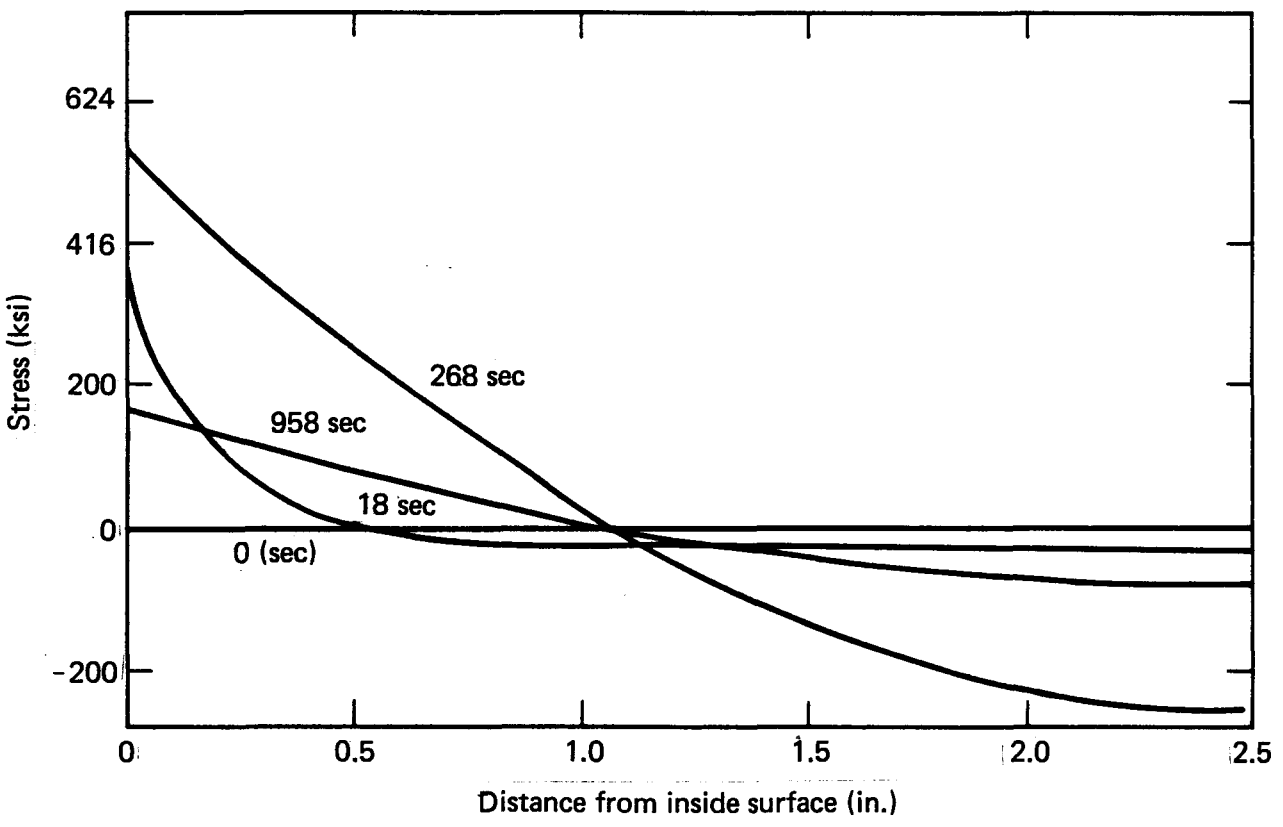

FIG. 3-1. Typical stress distribution for hot leg.

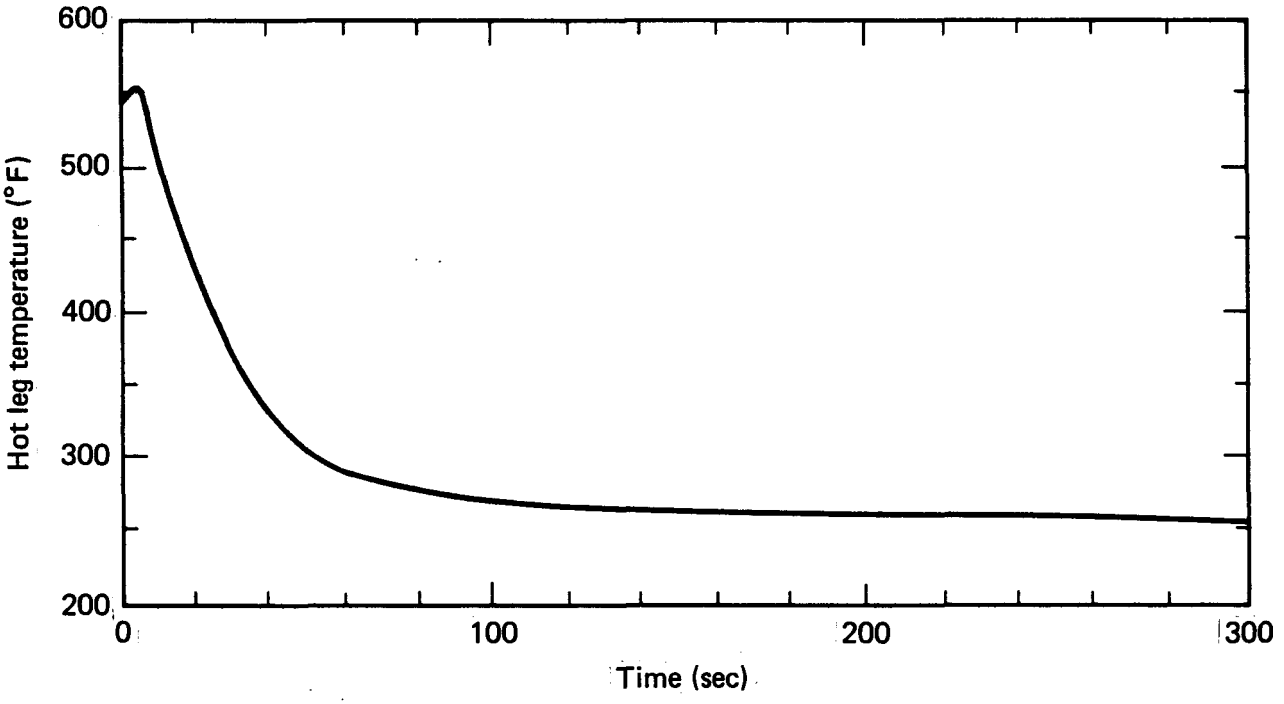

FIG. 3-2. Steam line break from no-load transient.

Table 3-3. Maximum and minimum thermal radial gradient stress at the inside surface.

Transient	Cold leg				Hot leg			
	Time (s)	Max (psi)	Time (s)	Min (psi)	Time (s)	Max (psi)	Time (s)	Min (psi)
1	0	0	17998	-2737	0	0	17953.3	-3410
2	14389	2770	0	0	17865.9	3450	0	0
3	1020	783	0	0	0	0	1019.7	4327.4
4	0	0	1020	-783	1019.8	4342.9	0	0
5	250.1	1322	50.06	-4032	300.0	2212.1	29.77	-1528.6
6	49.98	4033.2	1321.9	250.2	29.50	1648.9	299.96	-2101.7
7	840.02	2136	36.001	-3435	820.0	9292.6	60.07	-1456.8
8	100.05	735.8	26.87	-10463	100.07	18103.8	26.9	-8023.7
9	140.41	633	5.68	-3794	150.0	6160.2	2250.0	-2825.8
10	13.67	13806.6	42.27	-981.7	45.07	34605.6	15.93	-1559.0
11	100.01	3296.3	15.91	-5071.3	100.98	14388.5	4.12	-4587.0
12	39.97	3020.0	6.99	-942.9	39.61	21317.5	0	0
13	50.1	74118.7	0	0	60.01	74870	4.99	-940.6

Table 3-4. Surge line maximum and minimum thermal radial gradient stresses at the inside surface.

Transient	Time (s)	Max stress (psi)	Time (s)	Min stress (psi)
1	116.7	1568.4	1399.8	-3.8
2	1394.2	5732.4	142.46	-7919.0
3	0	0	73.5	-9984.0
4	96.2	10992.0	0	0
5	77.7	21888.3	0	0
6	1522.3	30381.8	31.6	-14001
7	0	0	10.05	-19012
8	32.00	69.07	30.0	-21707

4.0 RESIDUAL STRESS ANALYSIS FOR GIRTH-WELDED PIPES

Pressure vessel and piping components are joined by welding. Welding innerently causes residual stresses due to thermal gradients associated with melting and cooling of the weld deposit and surrounding base metal. Residual stresses can be tensile or compressive and generally vary in magnitude throughout the region near the weld. Experimental and analytical studies indicate that the peak values of weld-induced residual stresses approach yield stress of the metal at room temperature. Tensile residual stresses can be detrimental to the service life of the pipe because of their association with cracking.

4.1 OBJECTIVE

The goal of this study is to estimate the residual stresses for three different girth-welded pipes. Residual stress values are computed with a finite-element thermal-stress-analysis model. Of particular interest are the axial residual stresses, because the predominant mode of pipe cracking seems to be circumferential cracking, which is associated with axial stresses.

The three girth-welded pipes for this study are identified in Table 4-1. These pipes range in diameter from 14.0 inches to 34.0 inches, with pipe thicknesses varying from 1.4 inches to 2.5 inches. The pipe material is 316 stainless steel. The material properties used in the temperature-dependent elastic-plastic thermal-stress analysis are the same as those used in Reference 5 except for the temperature-dependent yield stresses, which are shown in Table 4-2. The heat inputs for the welding were obtained from information on the welding specification sheets for these pipes. The heat inputs used in the computational model are given in Table 4-3.

4.2 APPROACH

Residual stresses due to welding can be evaluated either experimentally or analytically. Experimentally evaluating these residual stresses can be time-consuming and expensive for the pipes considered here. Obtaining the throughwall distributions of residual stresses necessary for a fracture

Table 4-1. Description of girth-welded pipes.

Pipe	Outside diameter (in.)	Thickness (in.)
Surge line	14.01	1.406
Cold leg	32.26	2.38
Hot leg	34.00	2.50

Table 4-2. Temperature-dependent yield stress for 316 stainless steel.

Temperature (^{o}F)	Yield stress (ksi)
50	39.0
300	37.0
550	33.0
750	29.0
1000	24.0
1300	19.3
1600	16.0
2150	2.0

Table 4-3. Welding heat input values.

Pipe	Layer	Welding Current (A)	Welding Current (V)	Heat Input (kJ/in.)	Welding speed (in./sec)	Interpass temperature (^{o}F)
Surge line	1	120	24	27	0.08	70
	2	120	24	27	0.08	300
	3-7	160	25	30	0.10	300
Cold leg	1	120	24	27	0.08	70
	2	120	24	27	0.08	300
	3-9	160	25	30	0.10	300
Hot leg	1	120	24	27	0.08	70
	2	120	24	27	0.08	300
	3-9	160	25	30	0.10	300

analysis requires many machining operations and computations. An alternative and economical approach to obtain residual stresses is to use an established analysis procedure to predict residual stresses. Such a procedure and some of its applications are described in References 5-11.

From these references, it can be seen that the computational modeling of residual stresses due to welding is not a straightforward procedure. The problem is complicated by elastic-plastic temperature-dependent material behavior, complex heating and cooling phases, and elastic unloading from an elastic-plastic state of stress. There are relatively few publications in the literature on predicting weld-induced residual stresses.

The computational approach used here is to represent the mechanisms causing residual stresses and residual deformations within a practical computational technique to obtain a useful engineering tool. Well-established computational techniques, such as the finite element method, are used. A degree of confidence in the computational model is obtained by comparing predicted results with data. The method can handle butt-welded plates, as described in Reference 6, and deformations resulting from the flame-forming process, as described in Reference 7. A study of girth-welded thin-walled cylinders with two passes is described in Reference 5. Treatment of thicker walled pipes with 7 to 30 passes is described in Reference 8. In addition, weld repairs of thick-walled pressure vessels with up to 1000 passes have been investigated.[9] In all of these studies good agreement between computed values and available data has been obtained for residual stresses and residual deformations. Thus computational modeling of residual stresses has developed beyond prediction to application; it is now possible to identify and evaluate new ways for controlling residual stresses due to welding. The following sections describe the computational model and the results and discuss how the results relate to available residual stress data.

4.3 COMPUTATIONAL MODEL

The computational model has two parts: a temperature analysis and an elastic-plastic thermal stress analysis. The model includes a representation of the geometries, material properties, and weld process. The finite element approach allows flexibility in representing various geometries and permits inclusion of complex material properties. Constitutive equations are temperature-dependent and elastic-plastic, and they represent unloading from an elastic-plastic state of stress. Parameters of the welding process are also included in the model in terms of the temperatures generated during the welding process. The method includes time-dependent behavior due to heating and cooling. Geometric parameters such as initial configuration, weld groove geometry, and weld bead geometry are included in the finite element representation. Finally, numerical procedures in this model have been selected to make the analysis efficient. The analysis is also easy to use because it is based on the finite element method and on procedures that are common to many computer programs.

4.4 RESULTS AND DISCUSSION

The geometries and heat inputs described in Tables 4-1 and 4-3 were used as input for the residual stress analyses. For each of the three pipes, four locations were selected to display the throughwall residual stress distributions. One location is at the weld centerline. Two other loctions are in or near the heat-affected zone.

Resulting axial and circumferential stresses for the 14-in. surge line are shown in Figs. 4-1 and 4-2. The results show compressive values for both the axial and circumferential stresses at the inner surface of the pipe. The next two pipes analyzed were the cold and hot leg pipes described in Table 4-1. The residual stresses at locations corresponding to the weld centerline, 0.5, 1.0, and 2.0 inches away from the weld centerline, are shown in Figs. 4-3 and 4-4 for the cold leg and in Figs. 4-5 and 4-6 for the hot leg. The results for these two pipes are similar because of their similarity in diameter and thickness. Also note that both the axial and circumferential residual stresses are compressive at the pipe inner surface.

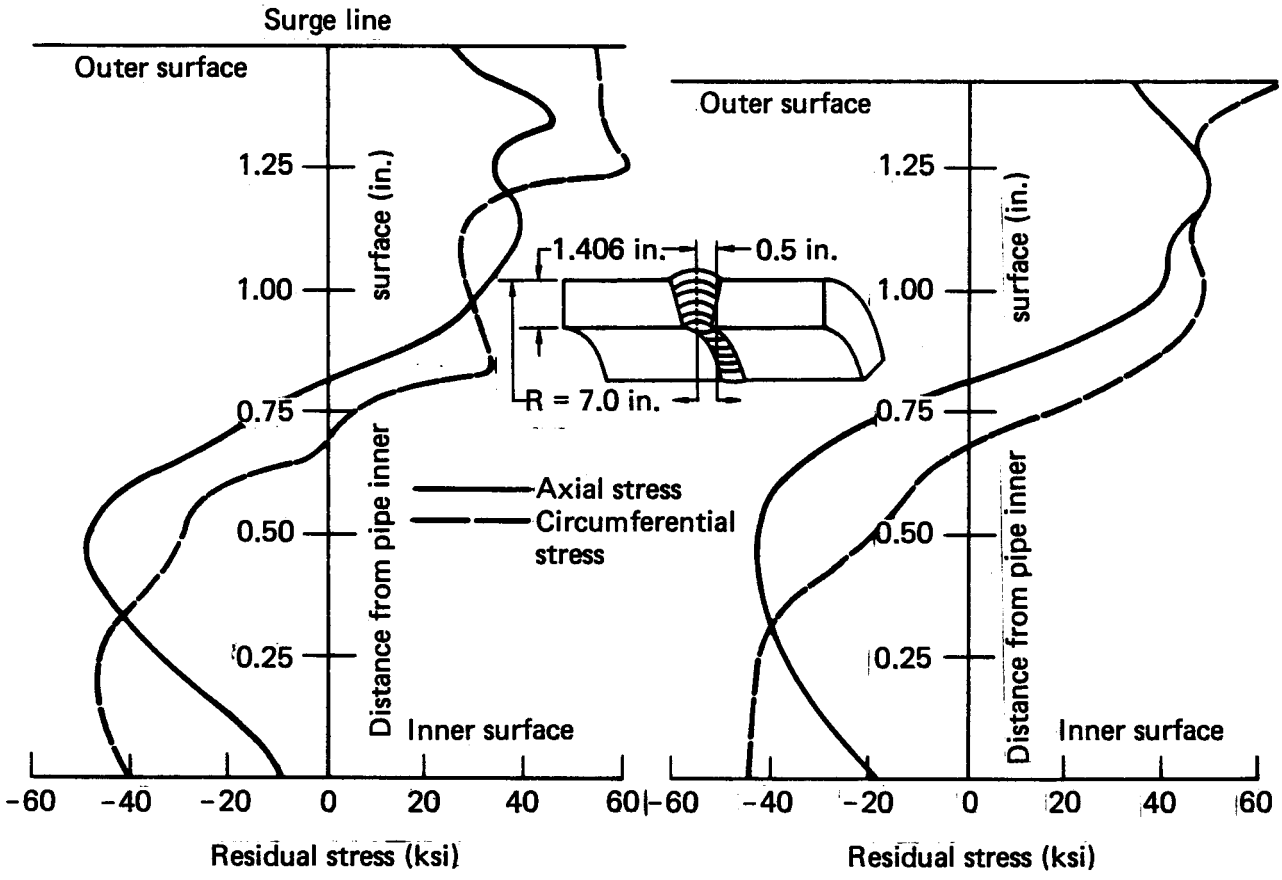

FIG. 4-1. Axial and circumferential stresses for welding a 14-in. surge line at cross sections on tne weld centerline and at 0.5 in. away.

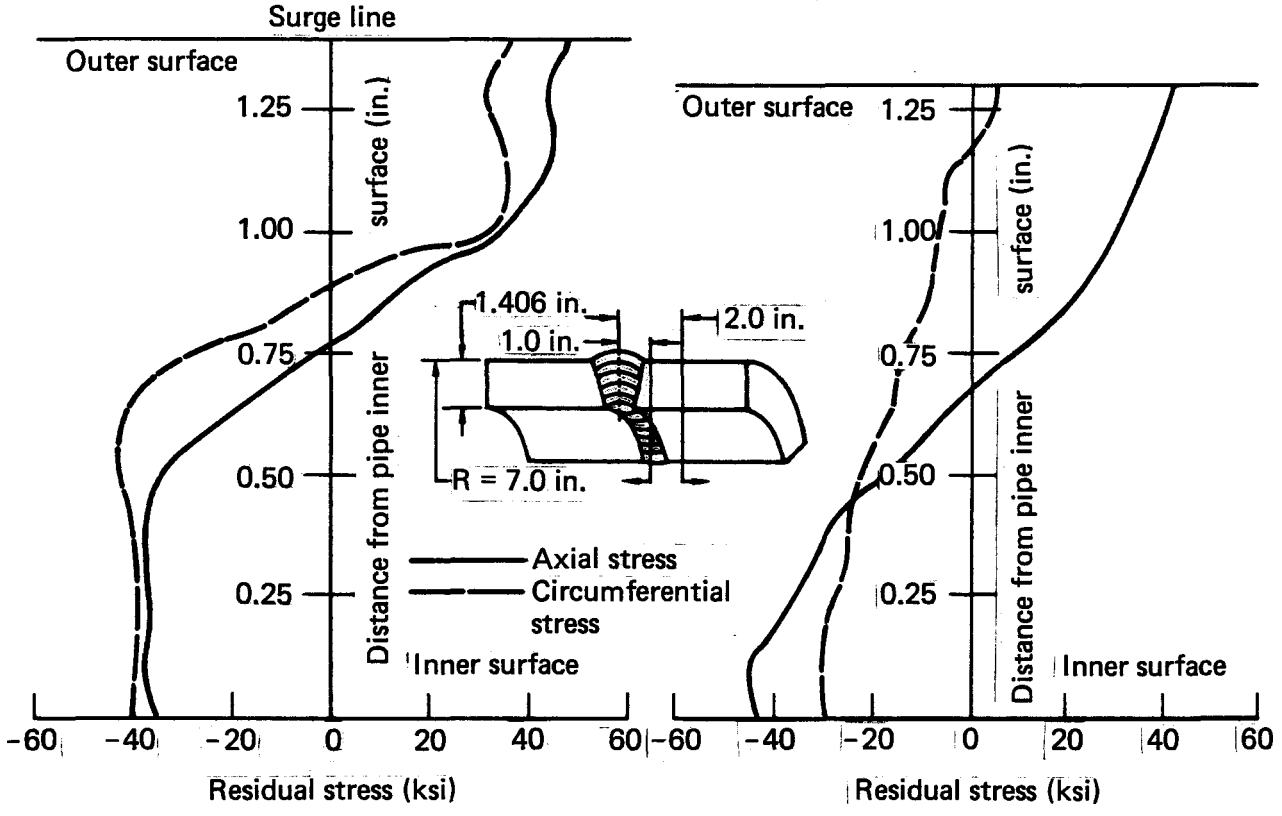

FIG. 4-2. Axial and circumferential stresses due to welding a 14-in. surge line at cross sections 1.0 and 2.0 in. from tne weld centerline.

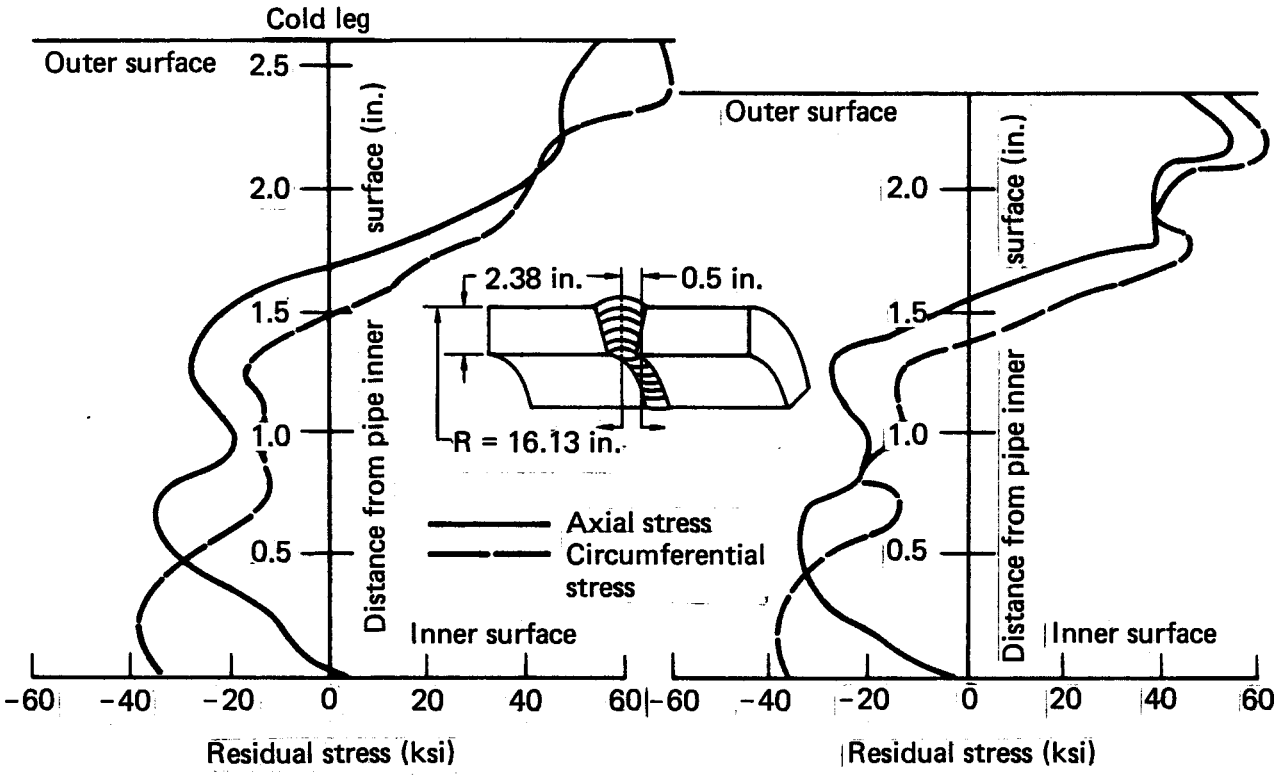

FIG. 4-3. Axial and circumferential stresses due to welding a 32.26-in. cold leg at cross sections on the weld centerline and at 0.5 in. away.

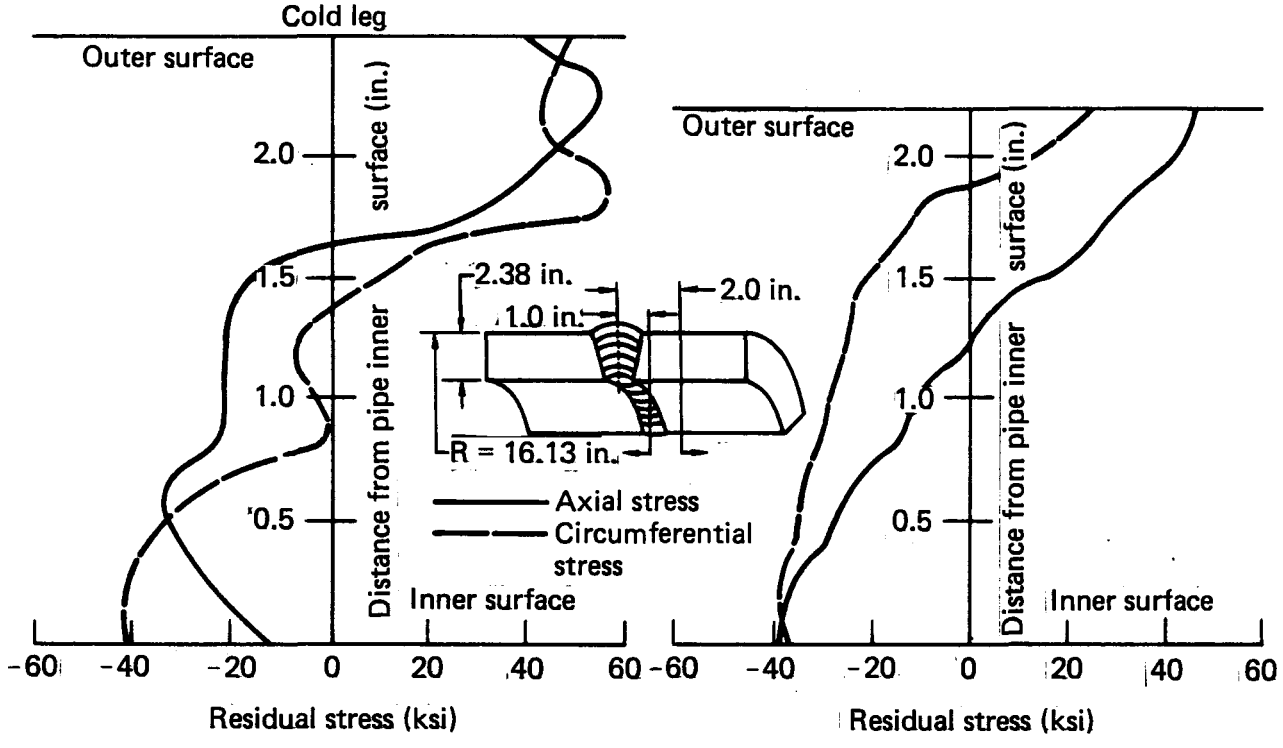

FIG. 4-4. Axial and circumferential stresses due to welding a 32.26-in. cold leg at cross sections 1.0 and 2.0 in. from tne weld centerline.

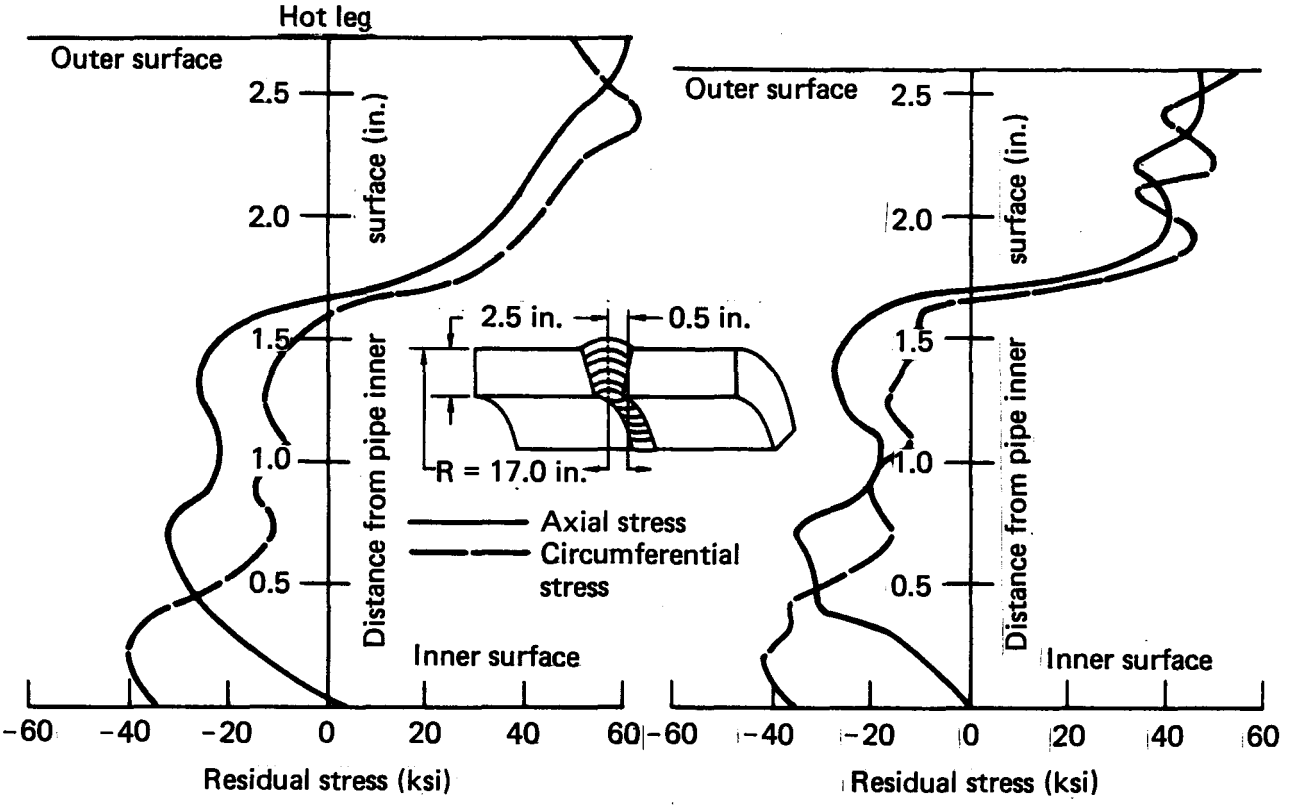

FIG. 4-5. Axial and circumferential stresses due to welding a 32.26-in. cold leg at cross sections 1.0 and 2.0 in. from the weld centerline.

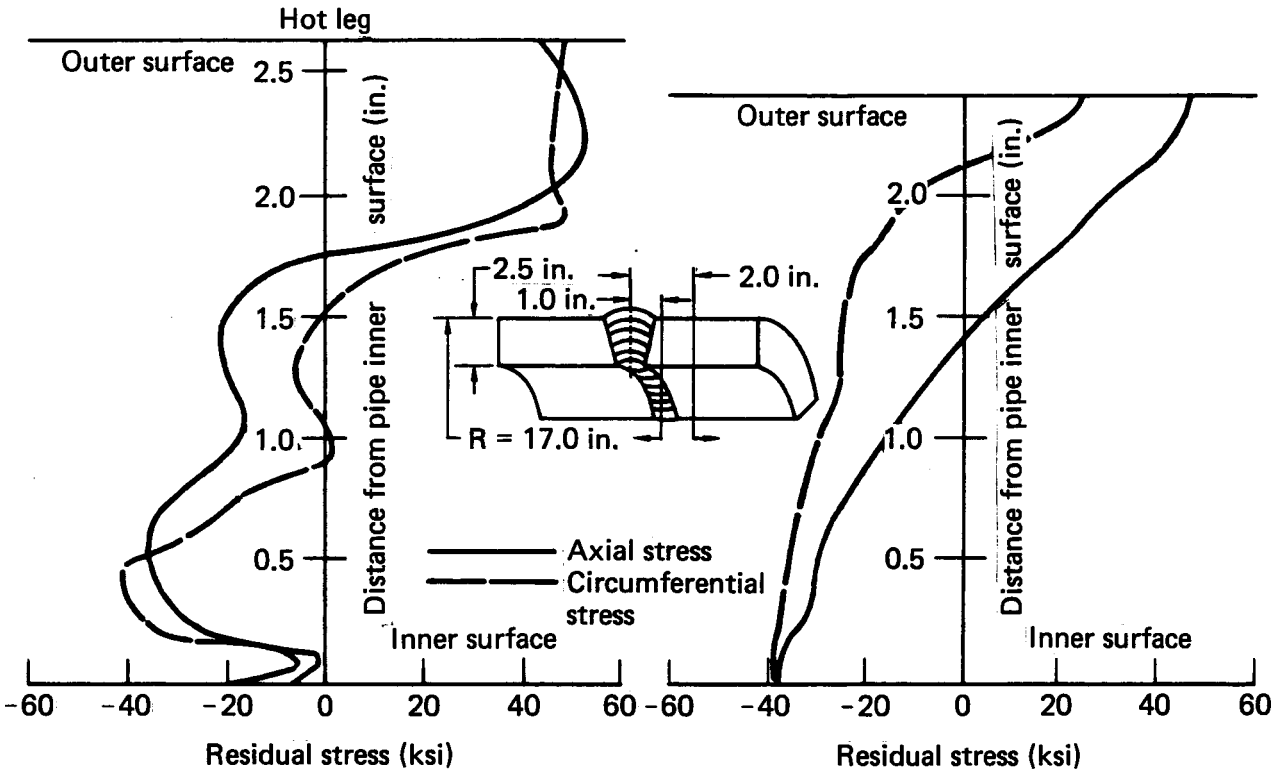

FIG. 4-6. Axial and circumferential stresses due to welding a 34-in. not leg at cross sections 1.0 and 2.0 in. from tne weld centerline.

The distributions of axial residual stresses along the pipe inner surface are shown for the three pipes in Fig. 4-7. The residual circumferential stress distributions are shown in Fig. 4-8. Both of these figures show compressive values near the weld fusion line for all three pipes.

Thus, the results obtained for all three pipes show compressive residual stresses on the pipe inner surfaces. These results are distinct from the results obtained for Schedule 80 pipes, which have generally shown tensile residual stresses on the inner surface. The main difference between Schedule 80 pipes and the three pipes considered in this study is that the Schedule 80 pipes have thinner walls than the pipes modeled here. The surge line in this study is Schedule 160 while the hot and cold legs are close to Schedule 120. This effect of pipe thickness on residual stresses has been observed analytically in studies of 4-in. and 10-in. pipes. It was found that the Schedule 160 pipes showed compressive weld residual stresses on the inner surfaces while the Schedule 80 pipes had tensile residual stresses.

The effect of thickness on residual stresses is also observed in terms of experimental residual stress data and computed values of stresses for a thick welded section.[11] The section referred to here is 6 in. thick and was welded as a weld repair. The data along with the values obtained from the computational model are shown in Fig. 4-9. It can be seen from this figure that the residual stresses at the inner surface were not tensile. Also, the stress distribution shown compressive stresses extending in the thickness direction of the vessel wall. Thus, this data and computed results provide further justification for the compressive stress behavior shown in Figs. 4-1 through 4-8.

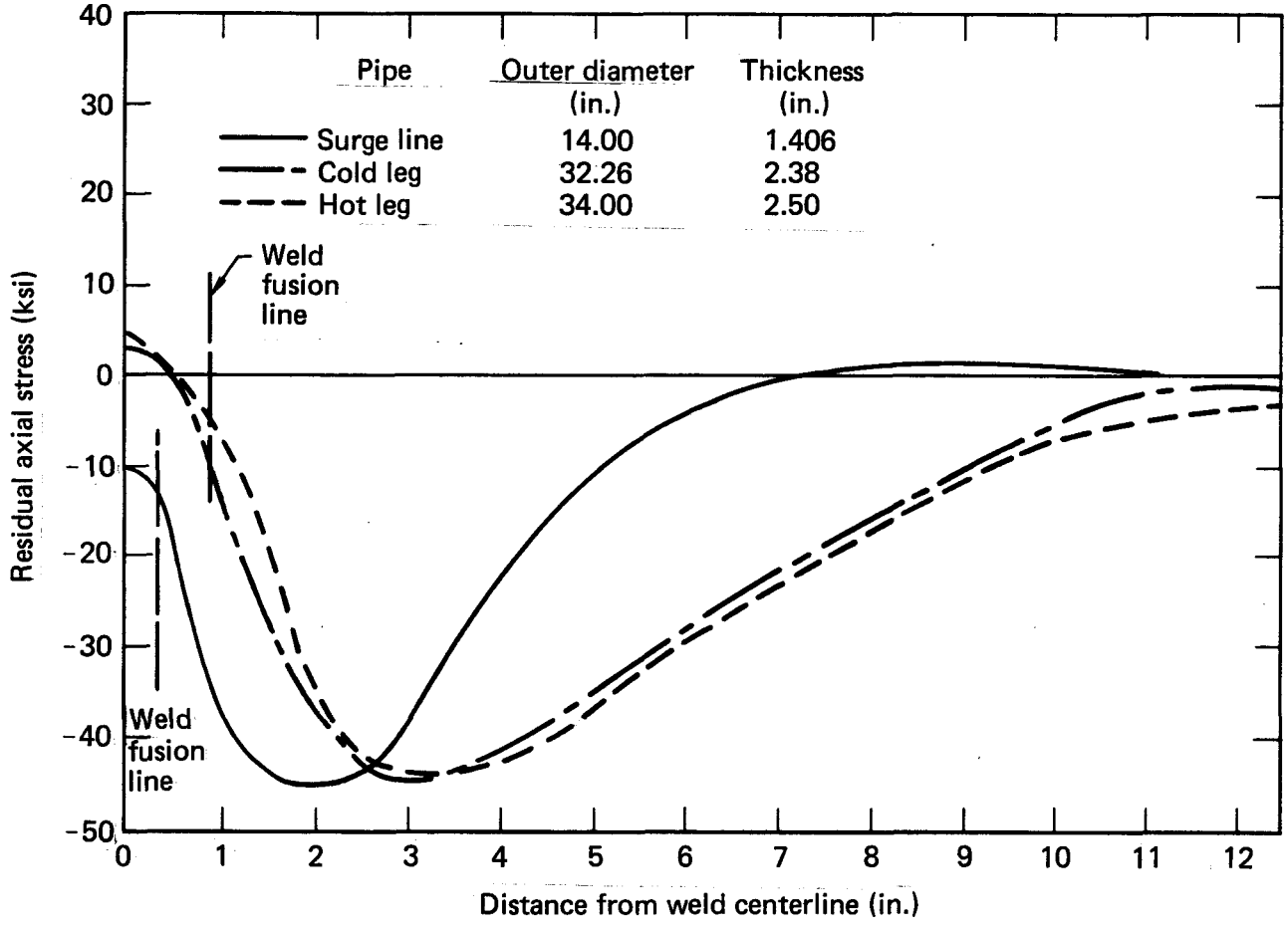

FIG. 4-7. Residual axial stresses along the inner surface of three pipes after welding.

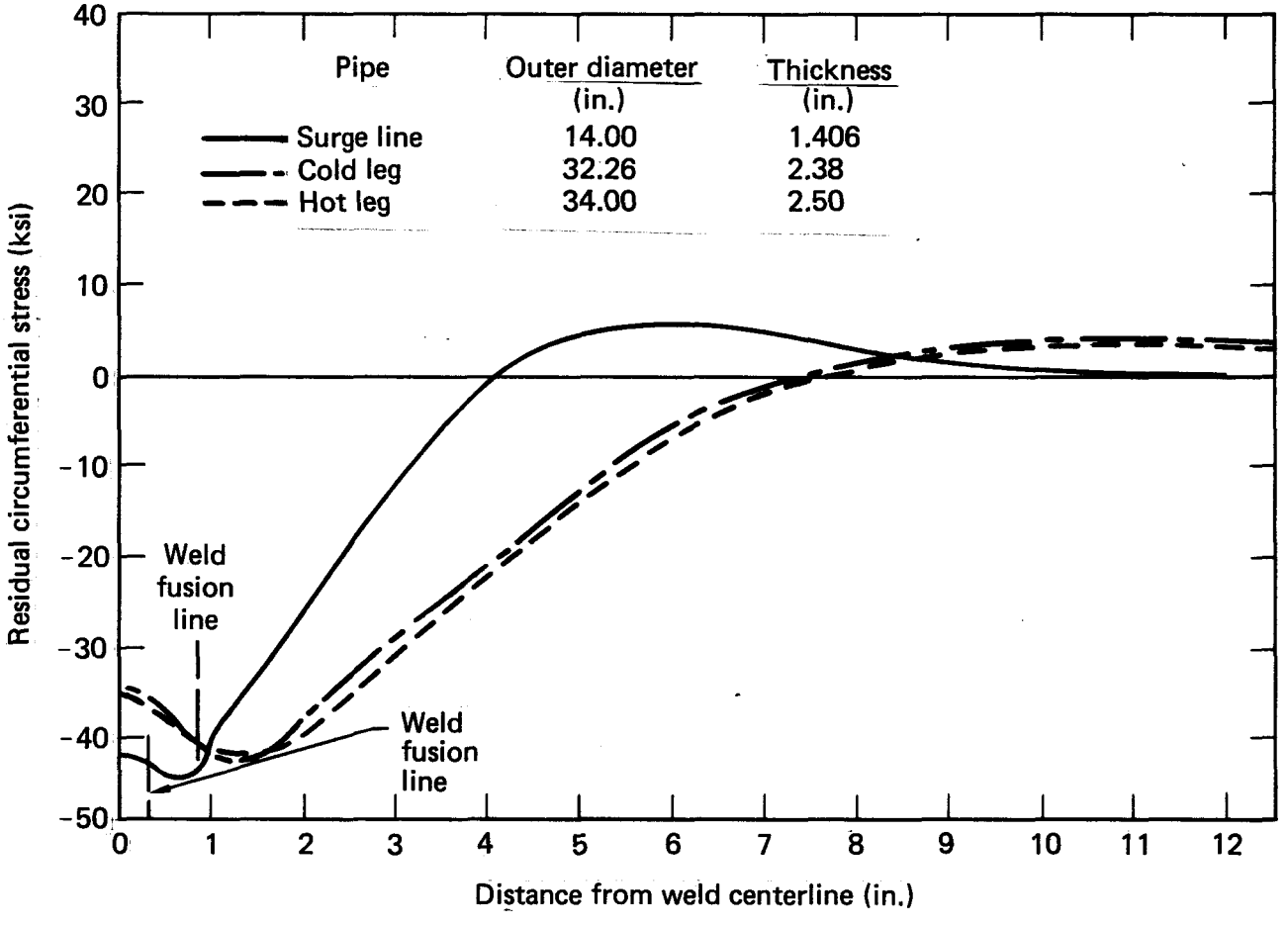

FIG. 4-8. Residual circumferential stresses along the inner surface of three pipes after welding.

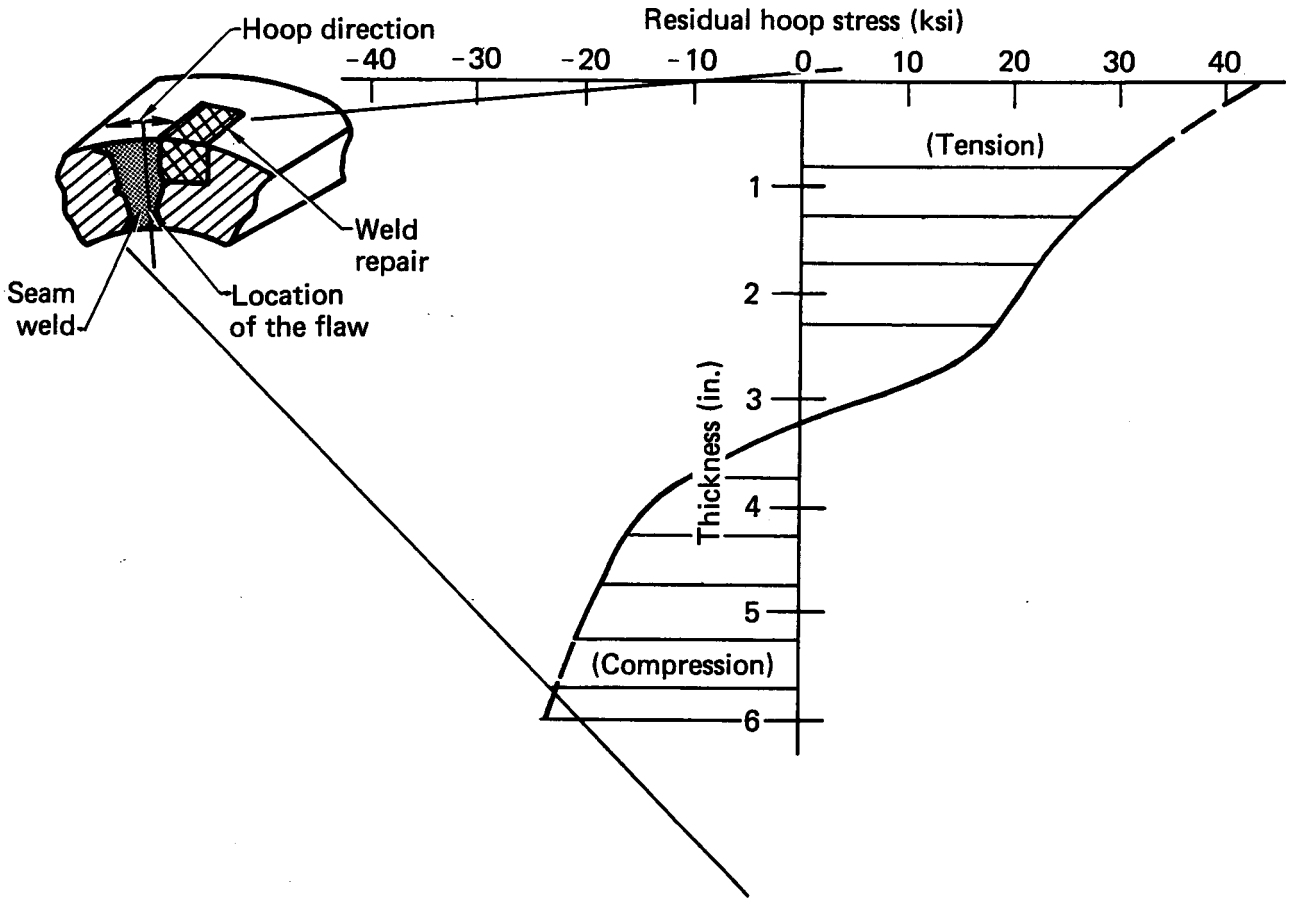

FIG. 4-9. Residual stress distribution at flaw location (From Ref. 7).

5.0 VIBRATION STRESSES

5.1 APPROACH

Vibration stresses in a piping system may be caused by rotation of equipment, by flow-induced vibration (such as vortex shedding, cavitation, or flushing), or by fluid pressure pulses. The importance of vibration stresses is dependent upon their magnitude. Excessive vibrational stresses can be detrimental to the piping system. The approach used to predict vibrational stresses in this study was to postulate a forcing function, perform a dynamic time-history analysis, and compare the results with the preoperational test data from the prototype Indian Point Nuclear Power Plant, which is very similar to the Zion plant (same thermal output and system configuration). Flow-induced vibration has not been included in this study.

The postulated forcing function was assumed to be a harmonic function:

$$Q = me\,\omega^2 \sin \omega t \qquad (5\text{-}1)$$

where Q = unbalanced force

m = rotating mass

e = eccentricity representing the center of mass and the axis of rotation

ω = rotating speed of equipment in radians per second.

This forcing function describes the forces resulting from imbalances in attached equipment and can be assumed to be input into the piping at a frequency that is some multiple of the running speed of the equipment. Other sources of vibration, such as flow-induced vibrations, were not quantified or included in the time-history analysis. They would become significant when their forcing frequencies correspond to a structural frequency and cause resonance.

The rotating mass (m) including the shaft, coupling, impeller, and fly wheel was calculated to be 36250 lb. from Westinghouse drawing No. 689J020. The eccentricity (e) is difficult to determine without experimental investigation. It is theoretically possible to balance the moving parts to

produce no unbalanced forces during rotation. However, in practice, some unbalance always exists. Its magnitude depends on factors determined by design, manufacture, installation, and maintenance procedures. In this study, e was assumed to be 6.5 mils. Because the design objective (per Westinghouse specification 677188) was to limit the vibration of the reactor-coolant-pump shaft to less than 13 mils (peak-to-peak composite) at the pump running speeds, 6.5 mils eccentricity was considered an upper-bound value. The operating speed (ω) of the reactor coolant pump is found to be 1190 rpm or 124.6 rad/sec from Westinghouse drawing No. 689J020. It was the only pump frequency used to calculate forcing functions in Eq. (5-1).

Substituting these values back into Eq. (5-1) yields the following forcing function used in the time-history analysis:

$$Q = 9437 \sin 124.4\, t. \qquad (5\text{-}2)$$

5.2 ANALYTICAL MODEL

The structural response of the reactor coolant loop piping to the postulated forcing function was determined by performing a time-history analysis that models loop 4 of the primary coolant loop. The model consists of the reactor, one steam generator, one reactor coolant pump, the pressurizer, and associated piping and supports. The model for loop 4 is basically the same as that developed by Sargent & Lundy in Volume 2 except that for the vibration study only loop 4 was modeled (the Sargent & Lundy model contained all four loops).

The reason for only model one loop in the vibration time-history analysis was to reduce the number of degress of freedom and thus, the computing costs. The results for loop 4 are considered representative of the other three loops.

Although this model only has loop 4 modeled in detail (i.e., close modal spacing and detailed equipment models), abbreviated portions of loops 1, 2, and 3 are included to account for their added restraining effect on the reactor. The abbreviated model contained the hot leg from the reactor out to the steam generator, where it was anchored, and the cold leg from the reactor to the reactor coolant pump, where it, too, was anchored.

Because the horizontal deflections of the steam generator at the point of the upper horizontal restraint were anticipated to be small, two time-history cases were run: one without the upper restraints and one with them. In the case where the upper restraints were excluded, the lower support model had to be modified.

The analytical model modification was found to be necessary due to the resulting instability of the steam generator when the upper horizontal restraint was removed. The modification consisted of adding four vertical restraints at the outside diameter of the steam generator in place of the one vertical support modeled by Sargent & Lundy. Four additional pipe members had to be added to transfer the loads from the center of the steam generator to its outside diameter. The torsional stiffness of the replaced one vertical support was accounted for by adding tangential truss members at the ends of two of the added pipe members.

5.3 ANALYTICAL RESULTS

The time-history analysis was performed using the SAP4 finite element code. The forcing function, 9437.0 sin 124.4 t, was applied through 20 cycles of load applied in both the axial and tangential directions simultaneously. The analyses were performed using 200 solution time steps. A 3% of critical damping was used. The analytical results were calibrated with available test results. The test used for calibration was performed by Westinghouse Electric Corporation for the Indian Point Unit 2 Power Plant.[12] Westinghouse measured loop vibrations at operating conditions during flow tests with several pump/temperature combinations. The data was analyzed using analog, hybrid, and digital computer techniques.

The Indian Point Unit 2 nuclear steam supply system is a Westinghouse pressurized water reactor owned by Consolidated Edison of New York. Like the Zion Station, the Indian Point Unit 2 plant has four primary coolant loops, each containing a steam generator, a reactor coolant pump, and loop piping as principal components. The support configuration is also very similar to that of the Zion plant.

The main ingredient for comparison is the deflection at the top of the steam generator. The 1-σ and 3-σ deflections from the test are given below; these deflections were calculated with an assumption of a normal distribution:

Radial deflection (1σ)	1.2 mils
Radial deflection (3σ)	3.8 mils
Tangential deflection (1σ)	2.2 mils
Tangential deflection (3σ)	7.0 mils

From the time-history-analysis results, the first natural frequency of the system is 7.2 Hz with shim and 2.4 Hz without shim. These frequencies result from the bending mode of the steam generator. This is in good agreement with the test results, which indicate a frequency of 6.9 Hz for the condition with shim and 2.4 Hz for the condition without shim.

The radial and tangential deflections at the top of the steam generator are as follows:

Radial deflection with shim	0.54 mils
Radial deflection without shim	0.506 mils
Tangential deflection with shim	0.37 mils
Tangential deflection without shim	0.75 mils.

These deflections are much lower than those found during preoperational testing at the Indian Point Power Plant. This indicates that the contribution from the higher reactor-coolant-pump shaft frequencies (i.e., at 39.7 Hz, 59.6 Hz, 79.4 Hz, etc.), the reactor-coolant-pumps blade-passing frequencies, and flow-induced vibration may be significant. In an attempt to account for the above-mentioned effects, the resulting stresses are scaled by the ratio of the measured deflections to calculated deflections. Since the ratio of the measured radial deflection to the calculated radial deflections is different from the ratio of the measured tangential deflection to the calculated tangential deflection, the average between the radial value and tangential value was used. The scaling factors for the conditions with and without shim are shown in Table 5-1. Because the deflections of the steam generator were

Table 5-1. Scaling factors for vibrational stresses.

Standard deviation	With shim	Without shim
1σ	4.06	2.65
3σ	12.97	8.4

represented as one or three times the standard deviation, Table 5-1 includes both factors. For the case of vibrational stresses with relatively low damping, the 3-σ deflection and scale factor gives the best estimate.

The 1-σ and 3-σ stresses for the conditions with and without shim are included in Table 5-2. The 3σ stresses are shown in Fig. 5-1. The maximum vibrational stresses are 0.581 ksi and 0.396 ksi with and without shim, respectively, at the cold-leg to reactor-coolant-pump welded joint. In a separate study conducted by the Steering Committee for Nuclear Energy,[13] the maximum vibrational stress was calculated to be 0.62 ksi based on the maximum observed pipe deflection during normal plant operation. This stress agrees reasonably well with the stresses that we have obtained from the dynamic analyses.

Because it is unlikely that the gap for the upper horizontal steam generator support will be closed due to vibrational loadings, the stresses from the condition without shim will offer the best estimate. The test report also indicates that the natural frequency of the steam generator is in the range of 2.2 to 3.2 Hz; this indicates that the upper steam generator support is not acting.

Table 5-2. Vibrational stresses.

Weld No.	Scaled bending stress from time history analysis			
	1-σ with shim	3-σ with shim	1-σ without shim	3-σ without shim
1	138	440	98	311
2	69	220	53	168
3	40	127	40	127
4	85	272	85	270
5	150	480	106	336
6	142	454	100	316
7	52	166	37	117
8	48	153	34	109
9	57	182	37	117
10	101	323	72	228
11	182	581	125	396
12	158	504	103	327
13	126	402	77	244
14	150	479	103	326

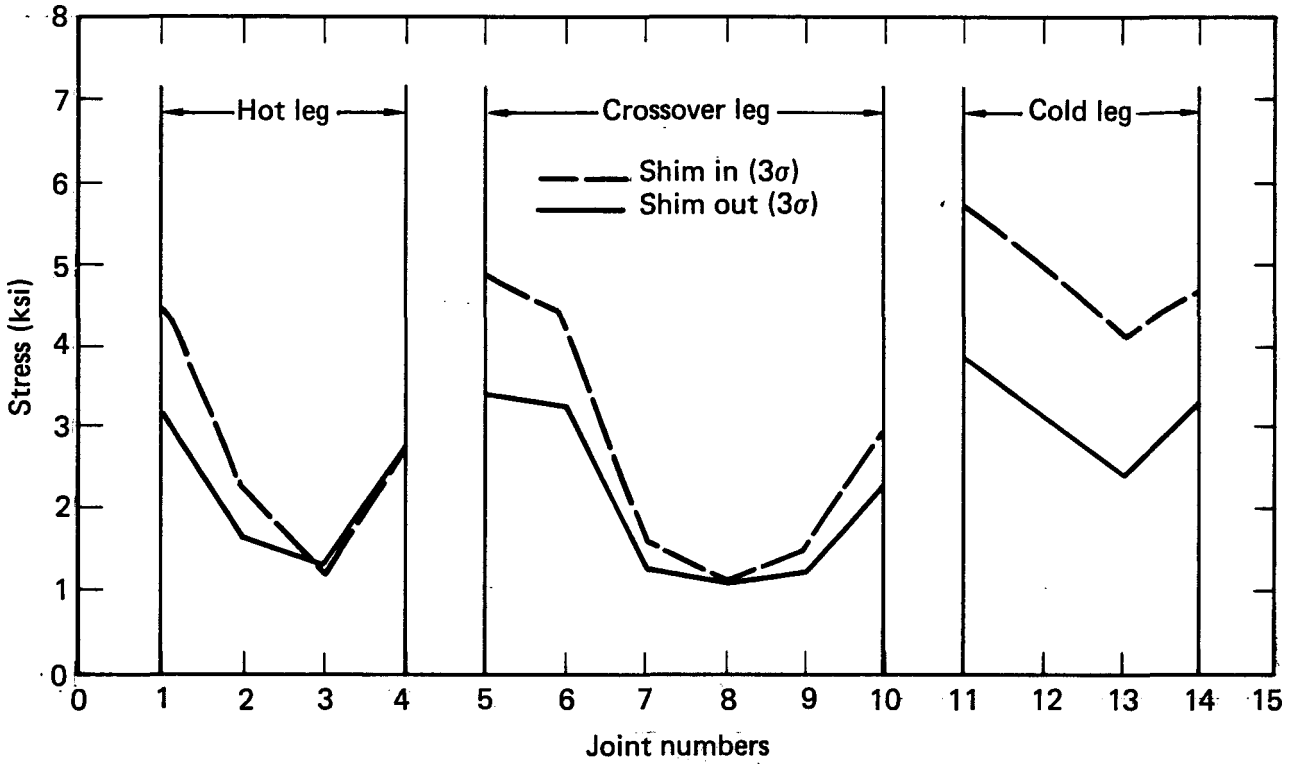

FIG. 5-1. Vibrational stresses at primary coolant loop welded joints.

Blank Page

REFERENCES

1. S. J. Sackett, Users' Manual for SAP4, A Modified and Extended Version of the U. C. Berkeley SAPIV Code, Lawrence Livermore National Laboratory, Livermore, CA, UCID-18226(1979).

2. W. C. Grangloff, An Evaluation of Anticipated Operational Transients in Westingnouse Pressurized Water Reactors, Westingnouse Electric Corp., Report WCAP-7486 (1971).

3. J. E. Brock and R. McNeil, "Speed Charts for Circulating of Transient Temperatures in Pipes, "Heating-Piping and Air Conditioning, Vol II, November, 1971.

4. H. S. Carslaw and J. C. Jaeger, Conduction of Heat in Solids, Second Edition, pp. 468-474, Oxford University Press, London (1959).

5. E. F. Rybicki, D. W. Schmueser, R. B. Stonesifer, J. J. Groom, and H. W. Mishler, "A Finite Element Model for Residual Stresses and Deflections in Girth Butt Weld Pipes," Journal of Pressure Vessel Technology 100, 149 (1979).

6. E. F. Rybicki, N. D. Ghadiali, and D. W. Schmueser, "An Analytical Technique for Evaluating Residual Deformations in Butt Weld Plates," presented at the ASME Winter Annual Meeting (November 27 - December 2, 1977), Atlanta, Georgia.

7. Y. Iwamura and E. F. Rybicki, "A Transient Elastic-Plastic Thermal Stress Analysis for Flame Forming," Journal of Engineering for Industry, Transactions of the ASME, February 1973, pp. 16-171.

8. E. F. Rybicki and R. B. Stonesifer, "Computation of Residual Stresses Due to Multipass Welds and Piping Systems," Journal of Pressure Vessel Technology 101, 149 (1979).

9. E. F. Rybicki and R. B. Stonesifer, "An Analysis of Weld Repair Residual Stresses for an Intermediate Test Vessel," presented at the Third U. S. Congress on Pressure Vessels and Piping, San Francisco, June, 1979.

10. E. F. Rybicki and P. A. McGuire, "A Computational Model for Improving Weld Residual Stresses in Small Diameter Pipes by Induction Heating," presented at the 1980 Pressure Vessel and Piping Technology Conference, August 11-15, 1980, San Francisco, CA.

11. E. F. Rybicki and R. B. Stonesifer, "An LEFM Analysis for the Effects of Weld-Repair Induced Residual Stresses on the Fracture of the HSST ITV-8 Vessel," Journal of Pressure Vessel Technology 102, 318-323 (1980).

12. Indian Point No. 2 Primary Loop Vibration Test Program, Westinghouse Electric Corp., Report No. WCAP-7920, September, 1972.

13. Report on a Parameter Study of the Probability of Leakage Due to Crack Growth in Primary Circuit Pipe Welds, Steering Committee For Nuclear Energy, Paris, August 20, 1979.

APPENDIX A: THERMAL TRANSIENTS

Blank Page

Table A-1. Heat up and cool down, not and cold leg temperatures.

Time (sec)	Heat up temperatures (°F)	Cool down temperatures (°F)
0.0	70.0	548.5
18000.0	548.5	70.0
20000.0	548.5	70.0

Table A-2. Unit loading and unloading at 5% rate, not leg temperatures.

Time (sec)	Heat up temperatures (°F)	Unloading temperatures (°F)
0.0	548.5	588.0
1020.0	588.0	548.5
1200.0	588.0	548.5

Table A-3. Unit leading and unloading at 5% rate, cold leg temperatures.

Time (sec)	Heat up temperatures (°F)	Unloading temperatures (°F)
0.0	548.5	540.0
1020.0	540.0	548.5
1200.0	540.0	548.5

Table A-4. Ten percent step load decrease, cold and hot leg temperatures.

Time (sec)	Cold leg temperatures (°F)	Time (sec)	Hot leg temperatures (°F)
0.0	588.0	0.0	540.0
29.4	593.0	27.1	550.0
50.0	593.0	50.0	554.0
100.0	590.7	64.7	554.0
135.0	588.0	100.0	550.0
250.0	579.8	150.0	546.0
500.0	580.0	200.0	542.0
1000.0	580.0	250.0	539.0
		1000.0	538.5

Table A-5. Ten percent step load increase, cold and hot leg temperatures.

Time (sec)	Cold leg temperatures (°F)	Time (sec)	Hot leg temperatures (°F)
0.0	588.0	0.0	540.0
29.4	582.6	27.1	530.0
50.0	583.0	50.0	526.0
100.0	583.0	64.0	526.0
135.0	585.0	100.0	530.0
250.0	595.0	150.0	534.0
300.0	596.0	200.0	538.0
400.0	596.0	250.0	541.0
		300.0	541.5

Table A-6. Large step decrease in load, cold and not leg temperatures.

Time (sec)	Hot leg temperatures (°F)	Time (sec)	Cold leg temperatures (°F)
0.0	588.0	0.0	540.0
60.0	593.0	5.0	550.0
120.0	589.0	36.0	552.0
240.0	572.0	120.0	553.0
720.0	528.0	126.0	553.0
820.0	520.0	480.0	542.0
1200.0	509.0	600.0	539.0
2000.0	509.0	720.0	537.0
		840.0	533.0
		1080.0	529.5
		1200.0	528.0
		1300.0	528.0

Table A-7. Loss of load from full power, cold and not leg temperatures.

Time (sec)	Hot leg temperatures (°F)	Time (sec)	Cold leg temperatures (°F)
0.0	588.0	0.0	540.0
10.0	591.0	5.0	545.0
27.0	614.0	10.0	551.0
32.0	588.0	20.0	567.9
50.0	566.0	23.5	573.0
90.0	528.0	26.5	574.1
100.0	525.0	33.3	574.0
1000.0	525.0	51.3	574.0
		60.0	557.0
		80.0	553.6
		100.0	544.0
		120.0	542.0
		300.0	542.0

Table A-8. Loss of off-site power, cold and hot leg temperatures.

Time (sec)	Hot leg temperatures (°F)	Time (sec)	Cold leg temperatures (°F)
0.0	588.0	0.0	540.0
150.0	564.0	5.0	552.0
418.0	574.0	140.0	540.0
843.0	574.0	590.0	538.0
2250.0	608.0	1500.0	538.0
3400.0	608.0		
9000.0			
1000.0			

Table A-9. Loss of flow in one loop, the last loop, cold and not leg temperatures.

Time (sec)	Hot leg temperatures (°F)	Time (sec)	Cold leg temperatures (°F)
0.0	588.0	0.0	540.0
16.0	593.0	4.2	520.0
20.0	558.0	10.0	501.0
25.0	493.5	13.5	496.0
45.0	472.0	16.0	496.0
80.0	482.0	20.0	510.0
100.0	488.0	23.5	520.0
1000.0	488.0	26.5	525.5
		30.0	533.0
		35.0	536.5
		40.0	539.5
		42.0	540.0
		45.9	540.0
		50.0	538.8
		80.0	538.0
		1000.0	528.0

Table A-10. Loss of flow in one loop, the other loops, cold and hot leg temperatures.

Time (sec)	Hot leg temperatures (°F)	Time (sec)	Cold leg temperatures (°F)
0.0	588.0	0.0	540.0
4.0	603.0	6.0	540.1
12.0	583.0	15.0	556.0
20.0	590.0	16.0	556.0
90.0	548.0	20.0	555.0
100.0	538.0	26.0	555.0
140.0	534.0	27.0	556.0
400.0	534.0	29.0	556.0
		40.0	549.5
		55.0	540.0
		70.0	534.0
		90.0	530.5
		500.0	530.0

Table A-11. Reactor trip from full power, cold and hot leg temperatures.

Time (sec)	Hot leg temperatures (°F)	Time (sec)	Cold leg temperatures (°F)
0.0	588.0	0.0	540.0
6.0	583.0	7.0	543.0
10.0	568.0	10.0	542.0
14.0	548.0	16.0	538.0
20.0	534.0	20.0	534.0
40.0	516.0	30.0	531.0
200.0	510.0	40.0	530.0

Table A-12. Steam line break from zero power, cold and hot leg temperatures.

Time (sec)	Hot leg temperatures (°F)	Time (sec)	Cold leg temperatures (°F)
0.0	548.5	0.0	548.5
5.0	551.5	4.0	500.0
8.0	548.5	7.0	450.0
22.0	400.0	28.0	350.0
40.0	330.0	46.0	300.0
60.0	290.0	50.0	290.0
280.0	251.0	280.0	251.0
1000.0	250.0	1000.0	250.0

Table A-13. Unit unloading at 5% rate, surge line coolant temperature and velocity.

Time (sec)	Normalized flow rate	Coolant velocity (ft/sec)	Time (sec)	Coolant temperatures (°F)
0	0.0	0.0	0	588.5
50	0.029	1.98	100	587.0
100	0.0	0.0	101	653.0
120	-0.007	0.477	1220	653.0
200	-0.006	0.41	1221	648.5
300	-0.009	0.613	1500	548.5
1020	-0.005	0.34	1501	653.0
1100	-0.052	3.54	1500	653.0
1220	0.0	0.0		
1280	0.010	0.68		
1500	0.0	0.0		

Table A-14. Unit loading at 5% rate, temperature and flow rates.

Time (sec)	Normalized flow rate	Coolant velocity (ft/sec)	Time (sec)	Coolant temperatures (°F)
0	0.0	0.0	0	653.0
50	-0.039	2.65	120	653.0
120	0.0	0.0	121	558.0
160	0.14	9.54	1200	648.0
240	0.004	0.274	1201	653.0
400	0.007	0.477	1400	653.0
500	0.0042	0.286	1401	588.5
1000	0.005	0.341	1600	588.5
1100	0.25	17.0		
1200	0.0	0.0		
1280	0.1	6.8		
1600	0.1	6.8		

Table A-15. Ten percent step load decrease, surge line coolant temperatures and velocities.

Time (sec)	Normalized flow rate	Coolant velocity (ft/sec)	Time (sec)	Coolant temperatures (°F)
0	0.02	1.36	0.0	588.5
10	0.083	5.66	10.0	590.0
40	0.0	0.0	40.0	595.0
50	-0.01	0.68	41.0	656.8
100	-0.02	1.36	80.0	649.4
200	-0.05	1.02	150.0	647.1
300	0.0	0.0	250.0	649.4
			300.0	653.0

Table A-16. Ten percent step load increase, surge line coolant temperatures and velocities.

Time (sec)	Normalized flow rate	Coolant velocity (ft/sec)	Time (sec)	Coolant temperatures (°F)
0	-0.02	1.36	0.0	653
10	-0.084	5.73	20	650
40	0.0	0.0	40	648
100	0.024	1.63	41	683
300	0.0	0.	75	587
			130	588
			200	592
			300	596

Table A-17. Large step decrease in load, surge line coolant temperature and velocity.

Time (sec)	Normalized flow rate	Coolant velocity (ft/sec)	Time (sec)	Coolant temperatures (°F)
0	0.5	34.0	0	588.5
20	0.0	0.0	20	591.0
30	-0.05	-3.4	21	653.0
40	-0.02	-1.63	1500	653.0
130	-0.02	-1.63	1501	509.0
160	-0.01	-0.68	1700	509.0
1200	-0.0	0.0		
1480	-0.02	-1.63		
1500	0.0	0.0		
1520	+0.04	2.73		
1630	0.0	0.0		

Table A-18. Loss of offsite power, surge line coolant temperature and velocity.

Time (sec)	Normalized flow rate	Coolant velocity (ft/sec)	Time (sec)	Coolant temperatures (°F)
0.0	0.0	0.0	0.0	588.5
4.0	0.22	14.99	6.0	588.5
6.0	0.0	0.0	7.0	653.0
10.0	-0.43	29.3	53.0	640.0
53.0	0.0	0.0	54.0	608.0
150.0	0.0	0.0	75.0	602.0
			135.0	574.0
			150.0	571.0

Table A-19. Reactor trip, surge line coolant temperatures and velocities.

Time (sec)	Normalized flow rate	Coolant velocity (ft/sec)	Time (sec)	Coolant temperatures (°F)
0	0.0	0.0	0	653
4	0.0	0.0	10	642
8	-0.75	51.1	30	630
15	-0.48	32.7	60	625
60	0.0	0.0	61	512
70	0.02	1.36	82	510
82	0.0	0.0	83	625
100	-0.01	0.68	100	625

Table A-20. Loss of load, surge line, coolant temperatures and velocities.

Time (sec)	Normalized flow rate	Coolant velocity (ft/sec)	Time (sec)	Coolant temperatures (°F)
0.0	0.0	0.0	0.0	588.5
17.0	1.0	68.2	5.0	590.0
24.0	0.0	0.0	10.0	592.0
34.0	-0.38	25.9	23.0	620.0
60.0	-0.12	8.20	25.0	668.0
80.0	-0.05	3.40	30.0	668.0
100.0	-0.02	1.63	35.0	639.0
120.0	-0.02	1.63	60.0	614.0
			100.0	604.2
			120.0	604.2

GLOSSARY

Artificial accelerogram

A numerically simulated acceleration time-history plot of an earthquake's ground motion.

Aspect ratio

Half-length-to-depth ratio of a semi-elliptical surface crack, $b/a = \beta$. The half length is measured along the surface of the pipe.

Availability

The percent of time that the reactor plant is actually in operation during its 40-yr life. For Zion, the estimated availability is 70%.

Boundary integral equation (BIE) technique

A mathematical solution of three-dimensional elasticity problems which divides a body's surface into elements and provides displacements and tractions at surface nodal points. Results are a set of simultaneous linear equations that are solved for the unknown nodal displacements or tractions.

BWR

Boiling water reactor.

Cold leg

Portion of the primary coolant loop piping which connects reactor coolant pump to reactor pressure vessel.

Conditional probability

If A and B are any two events, the conditional probability of A relative to B is the probability that A will occur given that B has occurred or will occur.

Confidence interval (estimator)

An interval estimator with a given probability (the confidence coefficient) that it will contain the parameter it is intended to estimate.

Containment

A concrete shell designed to house the NSSS, the polar crane, and other internal systems and components of a nuclear power plant.

Correlation

The relation between two or more variables.

Couple

To combine, to connect for consideration together.

Covariance

The expected value of the product of the deviations of two random variables from their respective means. The covariance of two independent random variables is zero, but a zero covariance does not imply independence.

Crossover leg

Portion of the primary coolant loop piping which connects the steam generator to the reactor coolant pump.

Cumulative distribution function (cdf)

A function that gives the probability that a random variable, X, is less than or equal to a real value, x.

DEPB

Double-ended pipe break.

Decouple

The opposite of couple; disconnecting two events.

EPFM

Elastic-plastic fracture mechanics.

Estimate

A number or an interval, based on a sample, that is intended to approximate a parameter of a mathematical model.

Estimator

A real-valued function of a sample used to estimate a parameter.

Fatigue crack growth

Growth of cracks due to cyclic stresses.

Flow stress

The average of the yield strength and ultimate tensile strength of a material. Approximate stress at which gross plastic flow occurs.

Fracture

See pipe fracture.

Girth butt weld

Circumferential weld connecting adjacent pipe ends. The girth butt welds referred to in this report are in the primary coolant loop piping.

Hazard curve (seismic)

The probability that one earthquake will generate a specified value of the peak ground acceleration in a time interval of specified length, usually one year.

Hot leg

Portion of the primary coolant loop piping which connects the reactor pressure vessel to steam generator.

Independent events

Two events are independent if, and only if, the probability that they will both occur equals the product of the probabilities that each one, individually, will occur. If two events are not independent, they are dependent.

Independent random variables

Two or more random variables are independent if, and only if, the values of their joint distribution function are given by the products of the corresponding values of their individual (marginal) distribution functions. If random variables are not independent, they are dependent.

LEFM

Linear-elastic fracture mechanics.

Large LOCA

Large loss-of-coolant accident. For the purpose of this report the large LOCA is equivalent to a pipe fracture in the primary coolant loop pipe. (See pipe fracture).

Leak-before-break situation

A pipe defect that grows to become a through-wall crack but is of insufficient length to result immediately in a complete pipe severance.

Load-controlled stress

Stress upon a pipe that cannot be relaxed by displacement. As such, the load is not relieved by crack extension. In this analysis pressure, dead weight, and seismic stresses are assumed to be load controlled.

Mean

(1). A measure of the center of a set of data. The sample mean of n numbers is their sum divided by n. (2). A population mean is a measure of the center of the probability density function. This is also called the mathematical expectation.

NSSS

Nuclear steam supply system.

OBE

Operating basis earthquake.

Operating stress

Stress in the piping due to normal operating loads, e. g., dead weight, pressure, start ups, etc.

Pipe fracture

A double-ended guillotine pipe break; also referred to in this report as a LOCA and a large LOCA. Refers to a circumferential pipe fracture in which pipe sections on either side of the fracture are completely severed from each other.

Pipe severance

See pipe fracture.

Poisson process

A random process, continuous in time, for which the probability of the occurrence of a certain kind of event during a small time interval t is approximately λt, the probability of occurrence of more than one such event during the same time interval is negligible, and the probability of what happened during such a small time interval does not depend on what happened before.

PRAISE

A computer code, Piping Reliability Analysis Including Seismic Events, developed to estimate the time to first failure for individual joints in a piping system. It is used to analyze the Zion 1 primary coolant loop. PRAISE is written in FORTRAN.

Primary cooling loop

Cold leg, hot leg, and crossover leg.

Probability density function (pdf)

A non-negative, real-valued function whose integral from a to b (a less than or equal to b) gives the probability that a corresponding random variable assumes a value on the interval from a to b.

PWR

Pressurized water reactor.

Radial gradient thermal stress

Axisymmetric stress in the pipe arising from temperature variations through the pipe wall thickness. In this report, the radial gradient thermal stress is a result of temperature transients in the reactor coolant.

Random variable

A real-valued function defined over a sample space.

Response spectrum analysis

A response analysis tnat estimates tne maximum response from response spectra.

RCL

Reactor coolant loop.

RCP

Reactor coolant pump.

Risk

Expected loss.

RPV

Reactor pressure vessel.

Sample space

A set of points that represent all possible outcomes of an experiment.

S factor

Stress factor used for fatigue analysis to account for multiple stress cycles.

Seismic nazard curve

See nazard curve.

SG

Steam generator.

Simulation

Numerical tecnnique employed to simulate a random event, artificial generation of a random process. Tne PRAISE computer code uses Monte Carlo Simulation to estimate tne probability of failure in nuclear reactor piping.

Soil impedance functions

Forces required to oscillate tne foundation tnrough unit displacements in different directions.

SSE

Safe snutdown earthquake.

Standard deviation

(1). A measure of tne variation of a set of data. Tne sample standard deviation of a sample of size n is given by tne square root of tne sum of tne deviations from tne mean divided by (n-1). (2). A measure of tne variability of a random variable. Tne population standard deviation is tne square root of tne variance; tne mean of tne square of tne random variable minus its mean.

Statistically dependent

Two events are statistically dependent if they do not fit the criterion for statistical independence.

Statistically independent

See independent events.

Stratified random sampling

A method of sampling in which portions of the total sample are allocated to individual subpopulations and randomly selected from these strata. The principal purpose of this kind of sampling is to guarantee that population subdivisions of interest are represented in the sample, and to improve the precision of whatever estimates are to be made from the sample data.

Stress corrosion cracking

Cracking due to the combined effects of stress and corrosion.

Stress intensity factor

A fracture mechanics parameter that describes the state of steam at the tip of a crack.

Surge line

Piping that connects pressurizers to the reactor coolant loop. In the Zion I PWR the surge line is a branch from the hot leg in Loop 4.

Time-history response analysis

A response analysis that estimates the maximum response from response spectra.

Transient

An event in the operation of the PWR that gives rise to a load in the piping over a specified length of time.

Uncertainty

Absence of certainty due to randomness of a random variable or lack of knowledge of the edf of a random variable.

Uniform hazard method (unm)

A procedure for estimating frequency of occurrence distributions for various ground motion parameters.

UT

Ultrasonic testing.

Variance

The mean of the squares of the deviations from the mean of a random variable.

ZPGA

Zero period ground acceleration; defines the size of an eartnquake.